WILEY ONLINE LIBRARY

Early View publication on wileyonlinelibrary.com
(issue and page numbers not yet assigned;
citable using Digital Object Identifier – DOI)

LASER & PHOTONICS REVIEWS

Laser Photonics Rev., 1–23 (2011) / **DOI** 10.1002/lpor.201100018

Abstract A century after the first optical cavity, coupled resonator optical waveguides (CROWs) were conceived as a new way to guide light on a photonic chip. Controlling chains of coupled resonators to let light propagate through, with a reduced speed and enhanced intensity, boosting light-matter interaction while keeping information undistorted: this was the fascinating promise of CROWs, but also one of the most ambitious challenges ever set for integrated optics. The first decade of the history of CROWs is discussed in this review, from the original idea to recent applications, panning through the technological platforms that have been employed to realize these structures. Design criteria and management issues, fundamental limits, and sensitivity to fabrication tolerances are discussed to make the reader aware of the performance of state-of-the-art CROWs and to provide a realistic perspective of future applicative horizons.

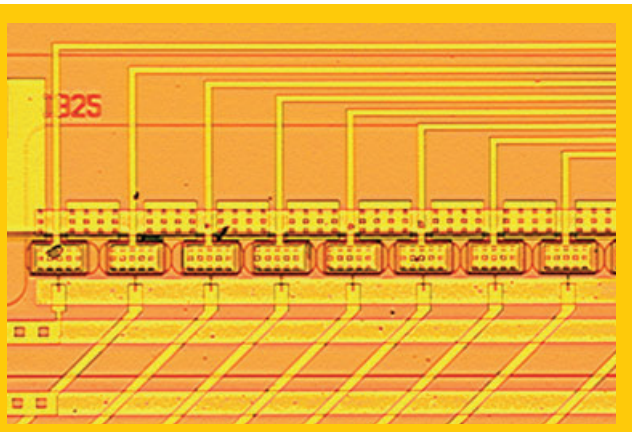

The first decade of coupled resonator optical waveguides: bringing slow light to applications

Francesco Morichetti[1,2,*], Carlo Ferrari[1], Antonio Canciamilla[1], and Andrea Melloni[1]

1. Introduction

Optical microresonators represent a subject of tremendous significance in modern photonics. The interest in tiny cavities able to confine a light field by resonant recirculation has been growing rapidly in many domains of optical science, from classical to quantum phenomena, from the linear to the nonlinear regime, from technologies and materials to applications in a variety of different fields [1–5]. Resonators indeed exhibit unique and intriguing properties that are widely investigated and exploited in optics, including the intrinsic spectral selectivity and the inherent infinite time response, as well as the capability of trapping light and enhancing the optical power at resonance, strengthening light-matter interaction, and boosting nonlinear effects.

When several resonators are coupled, the frequency and time domain behavior, as well as the design flexibility, are further enriched with respect to a single cavity, leading to complex and flexible systems that open unmatched opportunities in both the investigation of physical phenomena and their applications [3, 4, 6, 7]. In principle, any kind of cavity, independently of the shape and the technology, can be cascaded according to different topologies and synthesis algorithms, in order to tailor the desired response. However, among the various options available, microring resonators have been demonstrated so far to be the most flexible and well-established resonant building blocks for photonic circuits [4, 5, 7], while coupled resonator optical waveguides (CROWs), formed by chains of directly coupled cavities, have emerged as some of the best-performing and promising structures for a wide variety of applications, ranging from optical filtering to slow light delay lines, from nonlinear signal processing to trapping of light [8–11].

In this review we discuss therefore the state of the art of microring resonator-based CROW structures, focusing on the most relevant achievements reported in recent literature. The aim here is not only to give an exhaustive overview of the capabilities, impairments, and performance of present devices, but also to point out the potential of this approach and to outline the future applicative scenarios for CROWs.

Section 2 provides a general introduction to single and coupled optical cavities, underlining the motivations leading to the choice of ring-based CROWs for a wide range of applications. In Sect. 3 the propagation of light in directly coupled ring resonators is described according to the Bloch theory for periodic systems. The spectral behavior, the slowdown effects, and the main properties of CROWs are discussed for both linear and nonlinear regimes. Section 4 then provides a thorough review of CROW structures based on rings that have been demonstrated so far on different material platforms and discusses the role of the technological issues in determining the performance and limits of these devices. Another key issue for the successful application of ring-based CROWs, discussed in Sect. 5, is a careful design of the structure parameters in order to address the main drawbacks of slow light propagation: the velocity mismatch with nonresonant waveguides and the enhanced sensitivity to nonidealities. Then, Sect. 6 discusses the most appealing and advanced applications for these kinds of devices, by reviewing the published experimental results. CROW

[1] Politecnico di Milano, Dipartimento di Elettronica e Informazione, via Ponzio 34/5, 20133 Milano, Italy
[2] Fondazione Politecnico di Milano, piazza Leonardo da Vinci 32, 20133 Milano, Italy
[*] Corresponding author: e-mail: morichetti@elet.polimi.it

structures based on rings have been demonstrated to have potential mainly as optical filters and delay lines in the linear regime, and as wavelength converters through cavity-enhanced four-wave mixing in the nonlinear regime. Finally, Sect. 7 outlines the future perspectives in this field of photonics, focusing on two intriguing applicative fields, the active domain and the dynamic regime, promising to push forward the potential of CROW structures.

2. From the ring to the CROW

The aim of this section is to explain why, among the available cavities, the ring is the most suitable resonator for integrated optics and why the CROW is the most convenient way to combine several cavities. For more details on the properties of single-ring resonators and in particular on their realization on a silicon photonic platform, the reader is referred to a focused review paper by W. Bogaerts et al. that is included in this issue.

2.1. Cavities and the ring resonator

The first optical resonant cavity dates back to 1899 when C. Fabry and A. Pérot published a paper on a new method for "spectroscopie interférentielle" [12]. The Fabry-Pérot interferometer remained for years the only practical way to realize an optical resonator, at least until the emergence of integrated optical technologies in the late 1970s. More recently, the outstanding research progress in micro- and nanotechnologies has led to the advent of new-concept cavity shapes and the realization of resonators able to confine light in a size comparable to its wavelength in a material (λ/n) [1–3, 13].

Resonators can be classified according to the light confinement mechanism – total internal reflection or photonic bandgap – or to the field pattern at resonance – traveling wave or standing wave – and their shapes and structures can be extremely different [1–5, 7]. Figure 1 shows eight types of high-quality single resonators reported in the last decade. From Fig. 1a to h the resonators have the shape of a ring [14], a disc [15, 16], a toroid [17, 18], a sphere [2], an annular Bragg grating [19, 20], a defect in a photonic crystal lattice [21], and a Fabry-Pérot cavity defined with trenches [22] and holes [23, 24]. Most of them are suitable for large-scale planar integration on photonic chips and have excellent and somewhat complementary characteristics.

The spectral characteristics of resonators are well known and the reader is referred to many available textbooks for comprehensive discussions [3–5, 7]. The quality factor Q is probably the most important parameter for a resonator and is defined as

$$Q = \omega_0 \frac{\text{Stored energy}}{\text{Power loss}} \simeq \frac{\omega_0 \tau_R}{K + 2\alpha L}, \qquad (1)$$

where ω_0 is the resonant angular frequency, $\tau_R = n_g L/c$ the cavity roundtrip time related to the group optical length $n_g L$ of the cavity, K the power coupling coefficient between the resonator and the external environment, and α the attenuation constant inside the resonator. The quality factor can also be defined as 2π times the ratio of the cavity lifetime τ over the period of the optical wave $2\pi/\omega_0$; that is, $Q = \omega_0 \tau = \omega_0/B$, the latter being the familiar definition related to the bandwidth B of the resonance.

From Eq. (1) it is evident that the quality of the guiding structure plays a crucial role in defining the characteristics of the resonator. The "best" cavity is likely to be the one with the highest value of n_g/α. For example, record quality factors of more than 10^9 have been demonstrated in microtoroids [25] and microspheres [26, 27], largely outperforming the maximum Q-factor ever achieved in other kind of resonators. This is not surprising because the sphere is the geometry with the minimum surface for a given volume. However, in practical applications, there are other issues, such as fabrication complexity, device integration, reproducibility, and ultimately cost, that all contribute to the choice of the most suitable resonator to be used. In view of

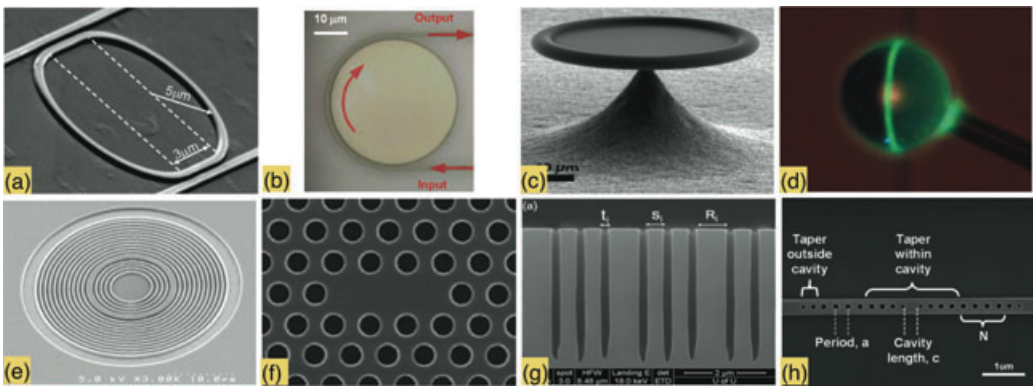

Figure 1 (online color at: www.lpr-journal.org) Images of optical resonators fabricated with integrated optical technologies: (a) ring (adapted from [14] ©2005 IEEE); (b) disc (adapted from [16] ©2010 IEEE); (c) toroid (adapted from [18] ©2008 Macmillan Publishers Ltd); (d) sphere (adapted from [2] ©2003 Macmillan Publishers Ltd); (e) annular Bragg grating (adapted from [20] ©2005 IEEE); (f) defect in a photonic crystal lattice (adapted from [21] ©2003 Macmillan Publishers Ltd); (g) Fabry-Pérot cavity defined with trenches (adapted from [22] ©2010 OSA); (h) chain of tapered holes (adapted from [24] ©2008 IEEE).

these considerations, microrings have emerged as the most established integrated optical resonators, being currently realized in several technologies and materials and employed in a very large number of applications [4, 5, 7, 28].

The history of the ring resonator began in 1969, when the idea was first conceived and appeared in the *Bell System Technical Journal* [29]. However, it was not until 1983 that one saw the first experimental realization in a silver-ion-exchange glass-based waveguide reported by researchers at the University of Glasgow [30]. Since then other fabrication trials followed, based on alternative technologies such as lithium niobate (1985) [31], silicon oxynitride (SiON) (1994) [32], and AlGaAs (1997) [33], up to the exponential growth of the last decade of the number of research activities exploiting ring resonators. Rings in almost every optical material, from polymers [34] to indium phosphide [35], from SiON [36] to chalcogenide glass [37], from silicon nitride [38] to silicon [39], have been explored with dimensions varying from centimeters down to micrometers [40] for applications spreading across several fields. Applications such as bandpass filters [36, 41], notch filters [42], phase shifters or delay lines [43], switches [44], modulators [45], lasers [46], sensing elements [47], frequency discriminators, optical differentiators and integrators [48], reference oscillators, optomechanic oscillators [49], and nonlinear-based devices such as wavelength converters [50, 51] and parametric oscillators [52] have been demonstrated and continue to attract the interest of both basic research and industry for their exploitation.

As in any optical cavity, the most appealing features of a ring resonator are the periodic spectral response and the intracavity field enhancement at resonance. The shape of the spectral response, with a periodicity given by the free spectral range $\mathrm{FSR} = c/n_g L$, is strictly related to the cavity optical length, attenuation α, and coupling coefficient with the external environment K. The intracavity field enhancement is proportional to the finesse of the resonator, defined as $F = \mathrm{FSR}/B$. According to Eq. (1) the lower are α and K, the higher are the Q-factor and the field enhancement and the narrower is B, which means a higher spectral selectivity. Although B and FSR can be chosen independently and optimized according to the specifications of the desired application and to technological constraints, the spectral shape cannot be modified arbitrarily, the single cavity being a first-order system, with a single pole and zero [6]. This implies that the bandwidth and the off-band rejection, as well as the intensity transmission response and the group delay are strictly related parameters that cannot be chosen independently. To achieve a higher flexibility of the frequency and time behavior, higher order systems must be considered or, in other words, more cavities have to be connected together. This is the subject of the next section.

2.2. Recent history of CROWs

The idea to connect together a number of resonators to shape the spectral response as desired was not originally conceived in optics, but it can be traced back to the beginning of the microwave era [53, 54]. Cavities can be coupled according to different topologies [6]: directly one to another (directly coupled resonators) [55], coupled in a parallel configuration [56], or coupled to a common bus waveguide [57]. Among these, the most suitable structure for tailoring the spectral response of filters, delay lines, and switches and for exploiting nonlinear phenomena is a chain of directly coupled resonators, which in optics is commonly referred to as a CROW [8, 10].

The term CROW appeared for the first time in 1999 in a theoretical paper by Yariv et al. [8] and about a year later the first experimental demonstration was provided using coupled defects in a photonic crystal waveguide [63]. Since then, CROWs have been realized using almost any of the cavities shown in Fig. 1. Fig. 2 shows examples of CROWs made by ring resonators [58], microtoroids [59], microspheres [60], square microresonators [61], and pho-

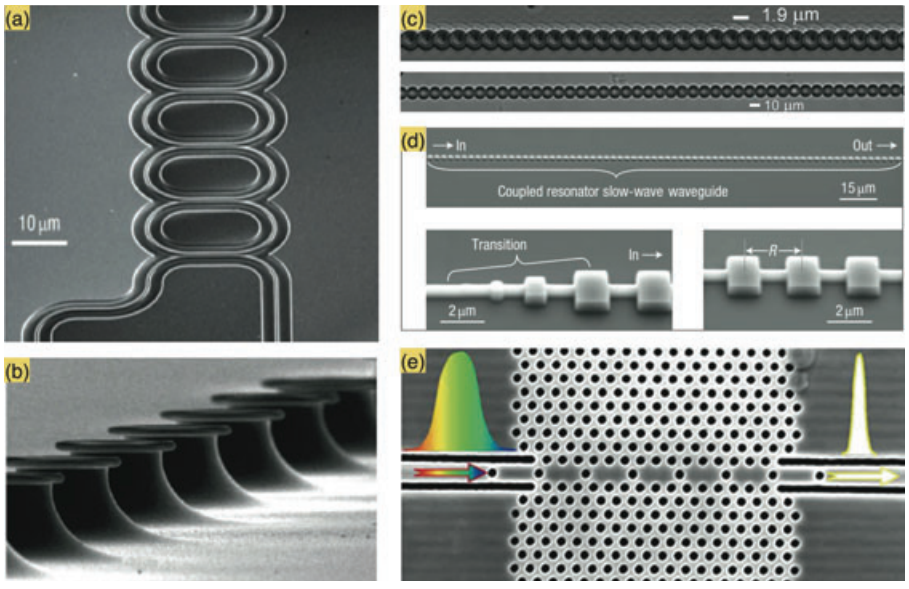

Figure 2 (online color at: www.lpr-journal.org) Examples of CROWs fabricated using (a) ring resonators (adapted from [58] ©2007 Macmillan Publishers Ltd), (b) microtoroids (adapted from [59] ©2010 IEEE), (c) microspheres (adapted from [60] ©2007 OSA), (d) square microresonators (adapted from [61] ©2008 Macmillan Publishers Ltd), and (e) photonic crystal cavities (adapted from [62] ©2002 IEEE).

tonic crystal cavities [62]. More recently, Bragg-defined Fabry-Pérot cavities [22] have also been demonstrated.

In order to realize good-quality CROWs, the Q-factor (i.e. the coupling coefficient between resonators) and the resonance frequency of all the resonators of the chain must be accurately controlled, as discussed in detail in Sect. 5. This is the main reason why ring-based CROWs have become the most popular, studied, and exploited structures in both linear and nonlinear regimes for a number of applications. Among the other alternatives to rings, only photonic crystal-based CROWs have, in some cases [64], comparable characteristics, but rings have demonstrated, up to now, to have superior quality in terms of optical performance, tunability, flexibility, and reproducibility [65]. For this reason, the following sections are focused on CROWs consisting of coupled rings.

An intriguing feature of CROWs is that the propagation of light is slowed down by a factor proportional to the finesse of the cavities. One of the first to realize the benefits of this effect was Taylor in 1999 [66], who proposed the exploitation of slow light propagation to reduce the velocity of light to that of a slower microwave field in traveling wave electro-optical modulators. The slowing down of light is now a well-recognized important field of research [11, 67] and CROWs are today one of the promising approaches to realize and manage this on photonic chips.

As in single resonators, the intracavity field intensity in a CROW is enhanced because of the conservation of the energy flux. This leads to a strong enhancement of any nonlinear effect, according to several powers of the slowdown factor (details are given in Sect. 3), making CROWs good candidates for the implementation of efficient all-optical devices [11, 68]. Although the benefits of nonlinear CROWs have been known since the pioneering work by Xu et al. in 2000 [9], followed by that of Melloni et al. in 2003 [10], the first experimental evidence of enhanced nonlinear efficiency was obtained only in 2009 [69, 70] (results are reported in Sect. 6.2). This demonstrates that the research in this field is still in its infancy. Ten years after their advent, the linear behavior of CROWs is now well assessed and understood and several technologies are sufficiently mature to realize high-quality long chains of ring resonators. From there, increasing research activity is needed and expected, leading to improvements in both basic understanding and in the realization of new functional devices.

3. Theory of CROWs

Independent of the type of resonator and technology, the concept underlying slow light propagation in CROWs is the forced recirculation of light through a number of coupled optical resonators [8]. Propagation in a CROW has been described either using the tight binding approximation [71], in analogy with the behavior of electrons in a periodic potential [72], or by means of the transfer matrix method [10, 73]. To point out the main properties of a CROW, it is convenient to refer to the ideal case of an infinitely long structure made of identical coupled resonators, as shown in Fig. 3a.

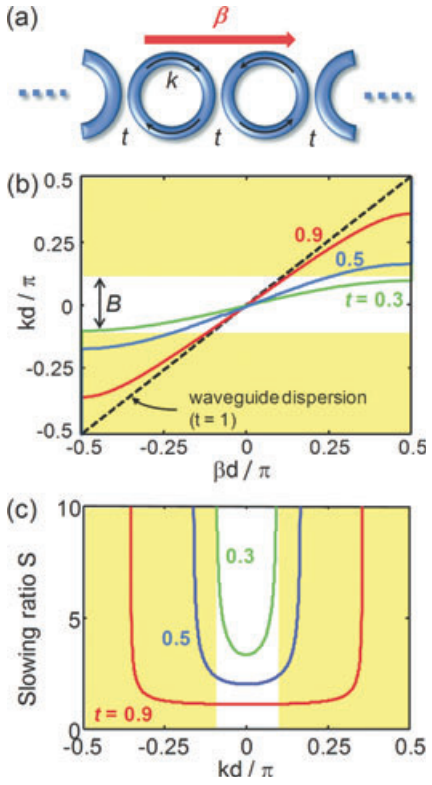

Figure 3 (online color at: www.lpr-journal.org) (a) Schematic of an infinitely long periodic CROW made of identical coupled resonators. (b) Dispersion diagram and (c) slowdown factor of an ideal CROW for coupling ratio t = 0.9, 0.5, and 0.3 between resonators. The dashed line in (b) shows the dispersion relation of the bare waveguide realizing the CROW.

In this arrangement, the propagation constant β obeys the Bloch theorem for periodic systems [53, 54] and satisfies the dispersion relation [10]

$$\cos(\beta d) = \frac{\sin kd}{t}, \tag{2}$$

where $t = \sqrt{K}$ is the field coupling ratio between resonators and $L = 2d$ is the physical roundtrip length of the resonators. The bare waveguide employed to realize the CROW has a wave vector $k = \omega n/c$, with n being the linear effective index. The dispersion diagram of an infinite CROW is shown in Fig. 3b for various values of t. Due to the periodicity of the structure, propagation is allowed only within a discrete number of passbands with bandwidth

$$B = \frac{2\mathrm{FSR}}{\pi} \sin^{-1}(t), \tag{3}$$

which are centered around the resonance frequency of the resonators and mutually spaced by $\mathrm{FSR} = c/2nd$. Inside each passband, the dispersion curve (solid curves) is strongly altered with respect to that of the bare waveguide (dashed black line) [74, 75], this resulting in a reduction of the group velocity of the CROW compared to that of the

waveguide according to a slowdown ratio [10]

$$S = \frac{\cos(kd)}{\sqrt{t^2 - \sin^2(kd)}}. \quad (4)$$

As shown in Fig. 3c, a higher S can be achieved in the tight binding regime ($t << 1$), but at the price of a bandwidth reduction. For a given value of t, i.e. for a given finesse F of the structure, S is a minimum at resonance ($S = 1/t$), then increases approaching the band edges where the group velocity ideally drops to zero. The strong frequency dependence of S indicates that, as in any slow-light system, the slowdown of the light in a CROW is associated with chromatic dispersion. Dispersion has a minimum in the middle of the passband where second-order dispersion vanishes and pulse propagation over tens of resonators can be achieved [74].

The expressions given above for the bandwidth and slowdown of a CROW hold also for finite-length structures with a sufficiently large number of resonators ($N > 6$), if properly matched to the input and the output waveguides [55, 76]. Issues related to the design and management of real CROWs are discussed in detail in Sect. 5.

Two main consequences arise from the slowdown of light. (1) Because of multiple roundtrips inside the resonators, the effective phase shift ϕ_{eff} experienced by the optical field propagating in the CROW is enhanced by a factor S with respect to the phase shift ϕ in a bare waveguide of the same length. This property makes CROWs of interest for the realization of phase-sensitive and phase-controlled devices as well as devices based on phase modulation [66, 77]. (2) Because of the conservation of the energy flux, the optical power P propagating inside the CROW is enhanced compared to the power P_{in} injected at the input, the average enhancement factor being equal to S. This second property makes CROWs particularly attractive for applications in the nonlinear regime.

In a material with third-order Kerr nonlinearity, the refractive index is perturbed by the local optical power P by an amount $\Delta n_{\text{NL}} = n_2 P/A_{\text{eff}}$, where n_2 is the nonlinear refractive index and A_{eff} is waveguide effective area. With respect to the linear case described by Eq. (2), in the nonlinear regime the dispersion relation of a CROW becomes [11]

$$\cos(\beta d) = \frac{1}{t}\sin\left[kd\left(1 + \frac{\Delta\omega}{\omega}\right)\right]. \quad (5)$$

Under the effect of nonlinearity, an intensity-dependent frequency shift

$$\Delta\omega = \frac{n_2}{n} c_n S \frac{P_{\text{in}}}{A_{\text{eff}}}\omega \quad (6)$$

occurs, which is proportional to the actual slowdown factor $S(\omega + \Delta\omega)$ of the CROW red-shifted by the nonlinearity. Owing to the frequency dependence of the slowdown factor, the spectral response of the CROW is not rigidly shifted, but is distorted by the nonlinearity. The coefficient c_n ranges from 1/2 to 2 depending on the type of resonators (ring or Fabry-Pérot) and on the number of different waves interacting inside the CROW [10].

Nonlinearity is also responsible for an additional phase shift of the propagating field. The nonlinear effective phase shift ϕ_{eff} may be related to the input power P_{in} as [57, 78]

$$\frac{d\phi_{\text{eff}}}{dP_{\text{in}}} = \frac{d\phi_{\text{eff}}}{d\phi}\frac{d\phi}{dP}\frac{dP}{dP_{\text{in}}} = c_n S^2 \gamma N d. \quad (7)$$

The first and the last derivatives, respectively, describe the above-discussed enhancement of the phase shift and of the intracavity power, and are both equal to the slowdown factor S; the second term of Eq. (7) expresses the dependence of the phase shift ϕ on the intracavity mean power P and is related to the nonlinear constant $\gamma = n_2\omega/cA_{\text{eff}}$ [79] and the number of cavities N. As a result, nonlinear propagation in a CROW is effectively described by an effective nonlinear constant [10]

$$\gamma_{\text{eff}} = c_n \gamma S^2, \quad (8)$$

showing that slow light propagation enhances the nonlinear phase shift according to a factor proportional to S^2.

An even higher enhancement factor is provided when frequency mixing phenomena occur inside a CROW [9, 67, 68, 80, 81]. For the sake of brevity, we restrict the analysis to the case of four-wave mixing (FWM), which, to date, is the only wave-mixing effect that has been experimentally observed in a CROW (see Sect. 6.2 for details of the experiment). The concept of FWM in CROWs is shown schematically in Fig. 4a. When an intense pump wave and a weak signal wave propagate at the central frequencies f_{p} and f_{s}, respectively, of two different CROW passing bands, an idler wave is generated within a third CROW passband at a frequency $f_{\text{c}} = 2f_{\text{p}} - f_{\text{s}} = M \times \text{FSR}$, where M is an integer. Inside the CROW, the power of all three waves is enhanced by S as well as the effective interaction length (or equivalently the interaction time). In the simplifying hypothesis of a slowly varying envelope, undepleted pump, small signals, and negligible self-phase modulation and cross-phase modulation effects, the power P_{c} of the converted wave after a length $L = Nd$ is [68]

$$P_{\text{c}}(L) = \gamma^2 P_{\text{p}}^2 P_{\text{s}} L_{\text{e}}^2 e^{-\alpha SL}\left(\frac{S^2+1}{2}\right)^2 \eta_\beta, \quad (9)$$

where P_{p} is the pump power, P_{s} is the signal power, L_{e} is the effective nonlinear length of the CROW, and η_β ($0 < \eta_\beta < 1$) is an efficiency parameter that includes loss α and phase matching terms. Two main results stem from Eq. (9). First, the absolute conversion efficiency $P_{\text{c}}/P_{\text{s}}$ grows quadratically with the nonlinear length of the CROW, i.e. the number of cascaded resonators, thus providing a substantial advantage with respect to FWM in single resonators [50, 51, 82–87]. Second, the maximum conversion efficiency is enhanced by the fourth power of S with respect to a bare waveguide with the same physical length L. The FWM conversion gain with respect to nonresonant FWM is shown in Fig. 4b versus the slowdown factor for different values of the product αL (for the sake of simplicity, the phase matched condition $\Delta\beta = 0$ is considered here). In the presence of loss, the theoretical gain reduces with respect to the S^4 curve (blue curve) and an optimum S exists that maximizes the gain

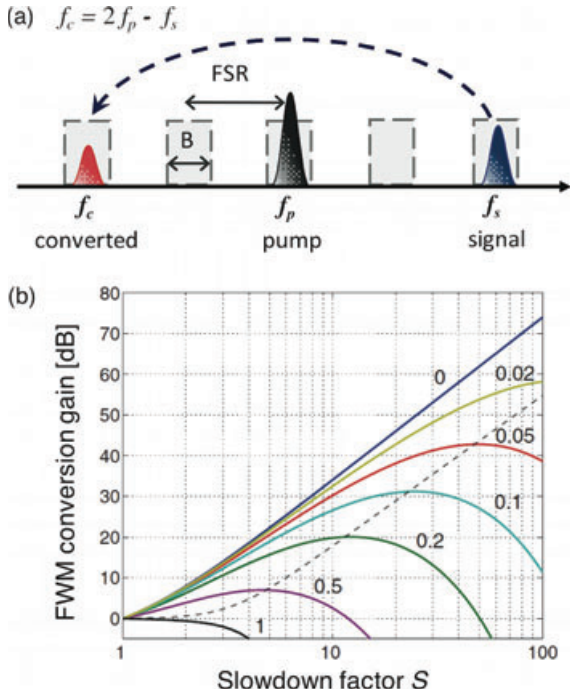

Figure 4 (online color at: www.lpr-journal.org) (a) Schematic of the FWM process in a CROW. The pump (f_p), signal (f_s), and idler (f_c) waves propagate each in three passing bands of the structure. (b) Theoretical FWM conversion gain of a CROW with respect to a bare waveguide of the same length for different values of the product αL. The gain is maximum along the dashed curve. (Image reproduced from [68] © 2008 OSA.)

(dashed line). However, the advantage of the CROW with respect to a simple waveguide is maintained as far as $\alpha L < 1$, independent of any other CROW parameter (B, FSR, and S).

More generally, slow-wave propagation enhances the efficiency of frequency mixing processes by S^q, where q is the number of optical waves involved in the mixing process [9, 80]. A contribution equal to S^2 is provided by the enhancement of the effective length, while an additional term S^{q-2} is related to the intracavity power enhancement experienced by all the interacting waves and takes into account the power reduction experienced by the converted field when leaving the CROW.

The combination of enhanced power intensity, spectral selectivity, and strong chromatic dispersion leads to a variety of intriguing nonlinear phenomena that can occur in a CROW. For a detailed analysis of these effects the reader is referred to chapter 10 of [11], which is dedicated to a theoretical and numerical investigation of nonlinear CROWs.

4. Technologies for ring-based CROWs

Since their first theoretical introduction [8], ring resonator-based CROWs have been realized by exploiting different technological solutions in terms of material platforms, waveguide structures, and circuit features.

The material platform affects the linear performances of a CROW mainly through the refractive index contrast Δn between the core and the cladding, since both the optical field confinement and the minimum acceptable ring radius decrease with it [91–93]. Generally speaking, therefore, higher contrast platforms enable not only a smaller footprint, but also a wider FSR: this enables a larger bandwidth B, once the finesse of the device is fixed, or a higher finesse and slowdown factor, once B is fixed. The drawbacks of increasing Δn, however, are a more challenging fiber-to-waveguide coupling and a stronger sensitivity to fabrication inaccuracies, i.e. higher losses and backreflections induced by sidewall roughness [94–96] and higher disorder effects due to dispersion of ring resonance frequencies and coupling coefficients [61, 65, 97, 98]. Moreover, Δn and the shape of the waveguide affect also the effective area A_{eff} of the propagating mode that, together with the nonlinear refractive index n_2 of the materials, determines the nonlinear performance of the platform [99, 100]. Finally, specific materials with particular features can be employed to enable techniques for optimization and reconfiguration of the CROW response or to improve the performances [101, 102], as discussed in detail in Sect. 5.

In recent literature, CROWs based on SiON [43, 88, 89], polymers (poly(methyl methacrylate) or PMMA) [90, 103], Hydex glass [41], and silicon-on-insulator (SOI) [58, 64, 65, 104–107] technologies have been demonstrated. Figure 5 shows images of some of these devices, whose figures of merit are summarized in Table 1. In this section the main properties of these technological platforms are reviewed, with the aim of pointing out which criteria should be taken into account in choosing the most suitable technology for a certain application.

Table 1 Figures of merit of state-of-the-art technological platforms used to realize CROW structures.

Platform	Δn (%)	Waveguide section (μm × μm)	$R_{\min}$ (μm)	$\text{FSR}_{\max}$ (THz)	$N_{\max}$	Footprint (μm^2/ring)	Roundtrip loss [a] (dB)	Tunability
SiON [88, 89]	4.5	2.2×2.2	300	0.1	8	4×10^5	0.2	Demonstrated
PMMA [103]	11	2.9×2.6	60	0.5	12	1.5×10^4	0.3	Possible
Hydex [41]	17	1.5×1.5	40	0.65	11	6×10^3	< 0.05	Possible
SOI [64, 108]	140	0.48×0.22	1–5	2–10	235	4–100	0.1	Demonstrated

[a] Ring length is about 4 mm in SiON, 380 μm in PMMA, 300 μm in Hydex, and 80 μm in SOI.

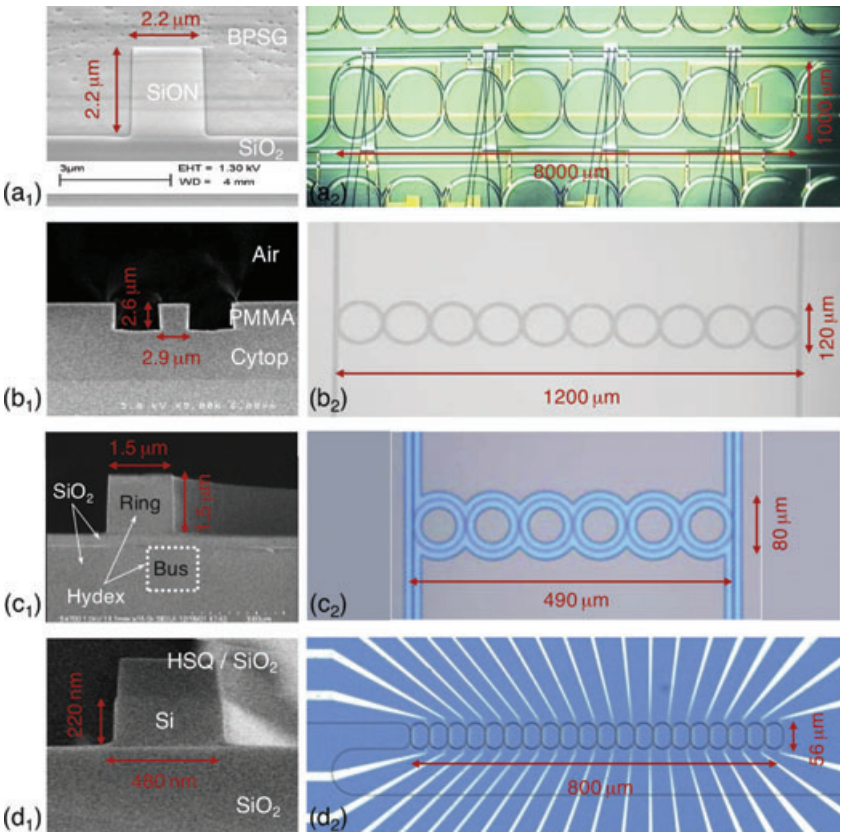

Figure 5 (online color at: www.lpr-journal.org) Images of (a_1–d_1) waveguide cross sections and of (a_2–d_2) CROW structures with N ring resonators realized on different platforms: (a) silicon oxynitride (SiON), $\Delta n = 4.5\%$, $N = 8$ (figures adapted from [88,89] ©2008 OSA); (b) polymer (PMMA), $\Delta n = 11\%$, $N = 10$ (figures adapted from [90] ©2006 IEEE); (c) Hydex glass, $\Delta n = 17\%$, $N = 6$ (figures adapted from [41] ©2004 IEEE and [85] ©2008 Macmillan Publishers Ltd); (d) silicon-on-insulator (SOI), $\Delta n = 140\%$, $N = 20$ (figures adapted from [64] ©2010 IEEE).

4.1. SiON technology

As representative of medium-index-contrast silica-on-silicon technologies, the SiON platform is at one extreme of the available alternatives. It was developed and used by Morichetti and coworkers to realize thermo-optically reconfigurable CROWs of up to eight rings [43, 88, 89], an image of which is shown in Fig. 5a_2. Single-mode SiON channel waveguides with 4.5% index contrast and $2.2 \times 2.2\,\mu m^2$ cross section (Fig. 5a_1) allow propagation loss down to $\alpha = 0.15$ dB/cm, coupling losses of 0.2 dB/facet (when butt-coupled with 3.5 µm small-core fibers), and bending radii down to 300 µm, resulting in a FSR of up to 100 GHz [43, 109, 110]. This technology combines fairly low roundtrip loss of 0.2 dB (including propagation loss, radiation loss in the bends, and excess loss in the directional couplers) with good system performance (see Sect. 6). The price to be paid with a moderate Δn is a limited bandwidth, roughly 10–20 GHz [43], and a minimum footprint of about 0.5 mm^2/ring. More details regarding the fabrication of SiON waveguides can be found in [111].

NiCr high-resistance metal strips were deposited on top of the waveguides to finely and independently control the resonance frequency of each ring by means of the thermo-optic effect, enabling one not only to compensate for fabrication inaccuracies (see Sect. 5), but also to easily reconfigure the spectral response and the induced delay of the CROW [43]. The gold strip lines supplying current to the heaters are visible in Fig. 5a_2. The results reported in [89] show a power consumption of 12.5 mW/GHz and a time response of the order of 150 µs.

4.2. Polymers

In order to overcome bandwidth limitations and to push forward the miniaturization and integration scale of CROW structures, platforms with higher Δn have been adopted. For instance, a polymer-based technology was employed by Poon et al. to realize CROWs consisting of up to 12 rings, an example of which is shown in Fig. 5b_2 [90, 103]. The PMMA waveguide, with a $2.9 \times 2.6\,\mu m^2$ cross section, shown in Fig. 5b_1 is patterned on a perfluoropolymer (Cytop) lower cladding, providing $\Delta n = 11\%$ with a simple fabrication process based on polymer spinning and direct e-beam writing. This technology enables the realization of CROWs with bending radii as small as 60 µm, a footprint reduction down to $120 \times 120\,\mu m^2$/ring, and an increase of the FSR and of the bandwidth up to 500 GHz and 50 GHz, respectively. As compared to SiON, these benefits are obtained at the expense of higher loss figures: 8 dB/facet coupling losses (with standard fibers) and rings with about 0.3 roundtrip losses. Although tunable CROWs in PMMA have not been realized so far, the tunability of integrated devices in polymer technology has been demonstrated by thermo-optic [112] and electro-optic [113] effects. Moreover, PMMA and other kinds of polymers show photobleaching properties that can be used to realize post-fabrication resonance trimming, as demonstrated for single-resonator devices [114].

4.3. Hydex technology

A further step towards higher index contrast is represented by Hydex technology, a proprietary glass material developed by Little et al. As in the example of Fig. 5c$_2$ [41], CROWs with up to 11 ring resonators were realized using a Hydex channel waveguide with $\Delta n = 17\%$ and $1.5 \times 1.5\ \mu m^2$ cross section, an image of which is shown in Fig. 5c$_1$ [85]. This waveguide allows bending radii down to 40 µm, reducing the ring footprint to only $80 \times 80\ \mu m^2$ (corresponding to a FSR of 650 GHz), and enabling bandwidths of the order of 50–100 GHz, suitable for managing high-capacity optical channels. Despite the high Δn, this platform guarantees ultralow propagation losses (down to 0.06 dB/cm), less than 1.5 dB/facet fiber-to-waveguide coupling losses, and a fine control of the technology, providing CROWs with a roundtrip loss of less than 0.05 dB and promising interesting system performance [41, 85].

Thermo-optic control of the resonance frequencies of each ring could be realized also on this platform with performance that, in principle, is the same as that for the other silica-based technologies. Although heaters on Hydex platforms have been reported [115] and used to control the resonances of multiring architectures [116], no reconfigurable Hydex CROWs have been demonstrated so far.

The Hydex platform also shows interesting nonlinear properties. Although its nonlinear refractive index n_2 is only 5 times larger than that of optical fibers, the high confinement produces an effective area $A_{\rm eff}$ roughly 40 times smaller, producing a nonlinear parameter γ that is about 200 times larger. Moreover, the very low loss figure enables high propagating power and long interaction length. These properties led to remarkable results for single Hydex rings also in the nonlinear regime [52, 85], although no results have been reported for CROW structures so far.

4.4. SOI technology

At the other extreme of the technological alternatives, a SOI platform with $\Delta n = 140\%$ produces the strongest mode confinement, allowing sub-micrometer waveguide cross sections [58, 65, 106], as shown in Fig. 5d$_1$, and bending radii down to 1 µm [40]. With respect to the previously described platforms, SOI technology enables photonic devices with unprecedented scale of integration ($4\ \mu m^2$/ring), as well as FSR (up to 10 THz), and bandwidth (up to 1–2 THz). The price to pay with SOI technology is the strong sensitivity to fabrication tolerances, leading to the need of a finely optimized process with nanoscale resolution, repeatability, and uniformity [58, 65]. An error of only 1 nm in the average waveguide width produces indeed a shift of the ring resonance of about 125 GHz [65]. Moreover, with state-of-the-art SOI technology, silicon nanometric waveguides exhibit propagation losses of about 1–2 dB/cm [117] and a challenging fiber-to-waveguide coupling that can be reduced down to 1–2 dB/facet only by means of complex mode-adapting structures [118–120].

Exploiting a SOI platform, silicon CROW structures were realized independently by several research groups at MIT [106, 107], IBM [44, 58, 104, 105, 108], and the University of Glasgow-Politecnico di Milano [64, 65]. CROWs with up to 235 ring resonators with bending radius of 6.5 µm, having a footprint of only 0.1 mm^2, were recently demonstrated [108] and represent a remarkable breakthrough in technological development. This experiment clearly pointed out the sensitivity of silicon CROWs to fabrication tolerances, even if waveguides are realized with nearly atomic-scale resolution and CROWs with a low finesse ($F \approx 2$) are considered. To be fully exploited, such devices need techniques and algorithms to compensate for fabrication tolerances, especially when a large number of resonators are cascaded and large slowdown factors are required, as discussed in detail in Sect. 5.

Thermo-optically tunable CROWs with up to 20 rings (Fig. 5d$_2$) were recently demonstrated [64, 65]. Due to the better thermo-optic properties of silicon, NiCr or titanium heaters on a SOI platform provide higher thermal efficiency, lower power consumption ($< 50\ \mu$W/GHz), faster time response (approximately 10 µs), and negligible thermal cross talk with respect to their counterparts on glass-based platforms [65, 121]. A great further advantage of SOI technology is that, by suitably doping the regions close to a rib waveguide, PIN junctions can be realized, enabling in this way a significantly faster resonance frequency control based on carrier injection and carrier depletion (the time response of which is of the order of 20 ps). However, the adoption of waveguides with a rib cross section weakens the mode confinement and bending radii for the ring resonators are larger with respect to fully etched silicon wire waveguides. This technique, already demonstrated in single-ring resonators [45], has not been applied to CROW structures yet, but could pave the way towards new interesting applications such as schemes to stop and trap light based on coupled resonator architectures [122–124].

The SOI platform is also promising for nonlinear applications. The silicon nonlinear refractive index n_2 is indeed 300 times higher and the mode effective area is roughly 1000 times smaller with respect to those of optical fibers, producing a nonlinear parameter γ that is about 3×10^5 times larger [99, 100, 125]. The main drawback for SOI nonlinear applications is represented by two-photon absorption [126] and free-carrier generation [127] effects. Their impact on CROW structures has been experimentally investigated [65] and is twofold: besides the induced extra losses, producing a saturation of the nonlinear effects, free carriers also cause a power-dependent refractive index change that can shift and distort the CROW transfer function, affecting its performance.

4.5. Other technologies

Besides these mature devices realized in established technologies, few other platforms have been exploited in pioneering works. III-V semiconductor compounds such as AlGaAs/GaAs and GaInAsP/InP were used [128, 129] to

demonstrate both passive and active CROWs of up to three rings, showing fairly good performance. The main attractiveness of this material platform lies in the promise of monolithic integration between active and passive integrated optical devices, opening the way towards advanced applications discussed in more detail in Sect. 7.

Coupled resonator filters with up to four rings were demonstrated also in silicon nitride technology [38, 130]. Despite the residual stress issues making its fabrication challenging, the silicon nitride platform is able to match a very high index contrast ($\Delta n \approx 50\%$) with low nonlinear property and two-photon absorption penalties, representing an attractive option for linear applications.

Finally, chalcogenide glasses [131], such as As_2S_3 and GeAsSe, are being exploited as promising materials able to guarantee high index contrast ($\Delta n \approx 60\%$) together with relatively low losses (of the order of 1–3 dB/cm) [132], strong nonlinear behavior together with weak nonlinear free-carrier effects [133, 134], as well as interesting photosensitivity properties enabling efficient post-fabrication trimming [102, 135]. The first preliminary results on chalcogenide CROWs have been recently reported [102, 136].

5. Design and management

Coupled resonator architectures are demonstrating their flexibility and potentialities in several fields of application. However, when dealing with slow light, one should carefully consider that almost every characteristic of the propagation is significantly altered by the slowdown. For instance, efficient injection of light from a bare nonresonant waveguide to a CROW is a key issue for the successful application of this kind of architecture and can be accomplished only by carefully designing the structure parameters. Moreover, the side effects due to material nonidealities or to tolerances in the fabrication process, as well as inaccuracies in the management of the structure are all expected to be as much pronounced as the slowdown factor S experienced by the optical field is high [97, 98]. Issues related to efficient light injection into a CROW and the effects of disorder are discussed in detail in Sects. 5.1 and 5.2, respectively.

5.1. Impedance matching of CROWs

It is well known that the characteristic impedance of a bare dielectric waveguide is proportional to the phase effective index n_{eff} whereas a periodic slow light structure has a characteristic impedance that is directly proportional to the group index n_{g}, which is its slowdown factor [97]. Therefore, periodic resonant waveguiding structures intrinsically have a higher impedance with respect to nonperiodic waveguides [137, 138] and if a chain of resonators is directly coupled to a "fast" nonresonant waveguide acting as a bus line, an impedance mismatch arises between the two, causing reflections at the coupling interfaces and hindering the light transfer efficiency. The mismatch appears as in-band intensity ripples in the spectral response of the devices and becomes more pronounced for higher slowdown factors of the CROW. This effect is clearly visible in Fig. 6a, showing the measured transmission at the output port of silicon CROWs made of identical racetrack resonators with radius 6.5 µm and field coupling coefficient $t = 0.398$, for an increasing number N of resonators [104]. The frequency of the in-band oscillations linearly increases with N, while the peak-to-peak amplitude decreases from 5 dB to about 2 dB because of the greater loss of longer CROWs.

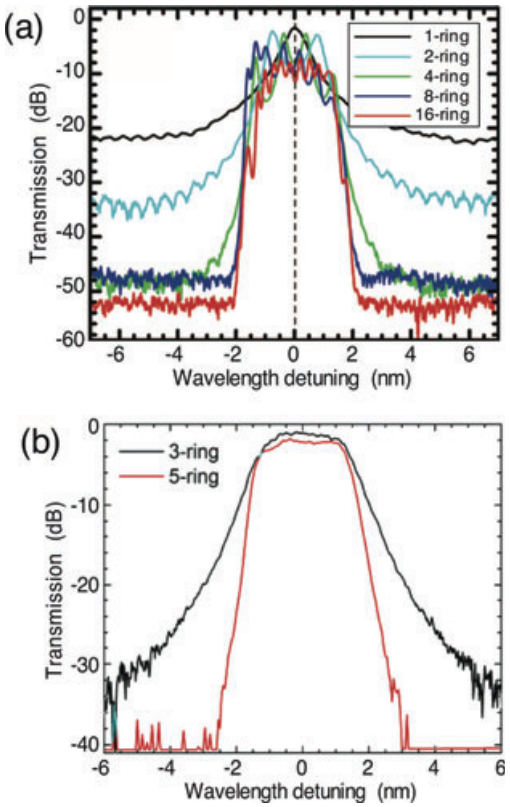

Figure 6 (online color at: www.lpr-journal.org) Effects of impedance matching in CROWs. Measured transmission at the output of silicon CROWs with increasing number N of ring resonators: (a) without impedance matching sections ($N = 1, 2, 4, 8$, and 16; adapted from [104] © 2006 American Institute of Physics); (b) with impedance matching sections ($N = 3$ and 5; adapted from [105] © 2007 OSA).

To achieve an in-band flat-top spectral response, impedance matching sections at the beginning and the end of the resonator chain must be suitably designed to have a progressive transition from a fast (low-impedance) to a slow (high-impedance) waveguide. The transition is typically managed by modifying the finesse (i.e. the inter-resonator coupling coefficients t) of the first (last) two or three cavities of the chain, while the central resonators are all kept equal. Several filter synthesis algorithms can be used to this end [6, 28, 55, 76, 139–141], which are mostly derived from microwave filter design theory and can be used to achieve a specific target intensity and phase response (e.g. with a Chebyshev, Butterworth, Bessel characteristic). The coupling coefficients t between resonators can be optimized

either by changing the length [43] or the gap distance [105] of the waveguides in the coupling sections, or by laterally shifting the rings [142]. The effect of CROW apodization is depicted in Fig. 6b, showing the measured transmission of silicon CROWs with a bending radius comparable to that used in Fig. 6a, but with a coupling coefficient that symmetrically decreases from the boundary to the center of the CROW. As a result, a flat-top passband with ripples smaller than 0.4 dB and insertion loss of only (1.8 ± 0.5) dB at the center of the passband is realized, while preserving an out-of-band rejection ratio of more than 30 dB.

The in-band reflection at a CROW input can be quantified by referring to the concept of return loss commonly used in filter nomenclature, where infinite return loss means zero reflection. A minimum level of reflection exists also in ideal structures with impedance matching sections, as stated by the Fano-Bode theorem [143], which sets a universal constraint between the bandwidth of a generic device and the maximum degree of impedance matching that can be achieved. The minimum bearable amount of return loss strongly depends on the application of the device; with properly designed structures return loss levels higher than 20 dB (i.e. light injection efficiencies higher than 99%) have been reached in fabricated CROWs [89, 106, 130] and are acceptable for a wide range of applications.

5.2. Effects of disorder in CROWs

Even with a proper impedance matching design, distributed backscattering and lumped backreflections related to structural disorder can have detrimental effects on CROW characteristics. Because of the sensitivity of slow-light devices to disorder (especially when S is high), several recent works have specifically investigated these phenomena, with the aim of finding a domain of realistic applications for slow-light waveguides. Disorder in slow-light optical waveguides has been demonstrated to be responsible for enhanced backreflections [144], limitations to the maximum achievable S [98, 145], and localization phenomena [61].

Deviations from the ideal design parameters of a CROW can consist of inaccuracies and deviations in the coupling coefficients between resonators (*coupling disorder*), misalignments of the resonances given by random variations in their optical lengths (*phase disorder*), and sidewall roughness [94]. All the sources of disorder produce similar effects on the CROW response; when a defect occurs, the periodicity of the structure is broken, the resonators act as partial reflectors, and the backreflected power decreases the return loss of the device. Moreover, the distributed backreflections can also give rise to marked time-domain distortions of modulated pulses propagating through the chain of resonators [97].

It has been predicted that in slow-light waveguides based on photonic crystals the backreflection caused by disorder increases with the square of S [146, 147] and with the square of the degree of disorder [148]; however, experimental results do not clearly confirm these predictions [144, 149, 150] and the actual phenomenon is very rich and deserves further investigation [151]. In CROWs it has been theoretically predicted that coupling and phase disorder effects scale quadratically with the group velocity reduction (i.e. according to S^2) and the results of pointed experimental investigations agree with the theoretical model [97]. Moreover, backscattering effects have been demonstrated to be coherently enhanced by resonant propagation in the cavities [95, 152–154].

Fig. 7 shows two examples of the effects of disorder in CROWs. Measurements of the spatial distribution of the optical field in a disordered silicon periodic structure at different wavelengths, depicted in Fig. 7a, show that, as the slowdown factor increases while approaching the band edge, localized patterns arise along the chain of resonators [61]. The localized and distributed backreflections given by disorder can also produce distortions in a modulated signal propagating through a CROW. Figure 7b shows the measured time traces of a 100 ps intensity-modulated pulse propagating through a CROW in the presence of weak and strong disorder that was intentionally induced and controlled in the

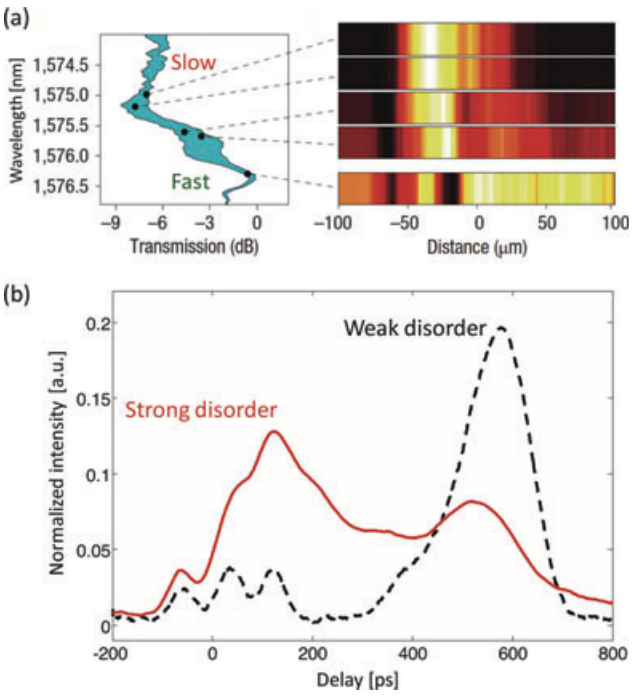

Figure 7 (online color at: www.lpr-journal.org) Effects of disorder in CROWs. (a) Measured transmission (left) and spatial field profiles (right) at different wavelengths near the band edge of a disordered silicon CROW structure. As the slowdown of the structure decreases with wavelength, extended nonlocalized field distributions are observed in the higher wavelength (fast) regions, while localized field distributions are observed in the lower wavelength (slow) regions. (Adapted from [61] © 2008 Macmillan Publishers Ltd.) (b) Measured time-domain effects of disorder on modulated 100 ps pulses propagating through an eight-ring glass CROW. In the presence of weak disorder (dashed curve) modest distortion is observed after propagation through the CROW (delay of approximately 600 ps), while in the presence of strong disorder (solid curve) a marked distortion given by distributed backreflections is observed. (Adapted from [97] © 2009 OSA.)

structure [97]. In the case of weak disorder modest distortion is observed and the pulse is clearly recognizable, while, if disorder is strengthened, the shape of the pulse is strongly affected by backreflections.

The tight dependence of disorder-related effects on the slowdown ratio makes the management of imperfections given by fabrication tolerances a key issue for successful exploitation of CROWs. On the one hand, it is not advisable to design structures with high slowdown factors; on the other hand, it is important to use post-fabrication tuning or trimming techniques to compensate for errors.

Indeed, recent experimental accomplishments [108] demonstrate that efficient propagation in very long chains (> 100) of coupled resonators can happen without the emergence of localization effects, if the structure has a very low slowdown factor ($S \approx 2$). For higher slowdown factors, phase disorder (i.e. unwanted spread in the resonance frequencies of the rings) becomes a dominant effect [65, 97] and needs to be actively compensated by using, for example, embedded thermal control of the resonances of the rings.

Another approach to cope with disorder-related issues and restore the proper behavior of CROWs would be to perform a post-fabrication trimming procedure of the structure parameters after testing the device with specific monitoring techniques to retrieve the phase errors [155,156]. To this end, photosensitive materials such as polymers and chalcogenide glasses have been successfully employed [101, 102].

However, there may also be other causes altering the structure parameters during operation, which are not related to fabrication inaccuracies. These effects cannot be eliminated with a permanent one-off trimming of the device response, but are time-varying processes that depend on the specific working conditions and need a dynamical and active control of the structure to be compensated. Nonlinear parasitic effects modifying the optical properties (e.g. the complex refractive index) of the material constituting the resonators, and hence the CROW response depending on the optical power flowing through it, belong to this category.

The presence and the strength of detrimental nonlinear effects are strictly related to the material properties and the optical field confinement in the waveguide. For example, two-photon absorption (TPA) and free carrier effects (free-carrier absorption and free-carrier dispersion) are the nonlinear effects that are the most likely cause of power-dependent structural disorder in silicon CROW structures [157, 158]. The power-dependent modification of the refractive index induced by TPA leads to a shift in the resonance frequencies of the resonators. However, the resonance shift varies strongly from cavity to cavity; propagation loss attenuates light intensity along the CROW and the optical power is locally enhanced according to the cavity finesse, which is not constant across the chain of resonators, but changes in the impedance matching sections. Since the optical power level along the CROW is neither uniform nor accurately predictable, TPA-related effects can give rise to phase disorder [65] and corrupt the proper behavior of the device.

The active management of CROW structures for disorder compensation and reconfiguration purposes is not a trivial task and the future development of automated tuning algorithms to achieve the target performance is a requirement towards the successful exploitation of CROW devices.

6. Applications

The linear and nonlinear properties of CROWs have attracted much attention for applications in a wide range of fields, spanning from signal processing devices for telecommunication and interconnect networks to optical sensors with enhanced sensitivity. The most appealing and advanced applications of CROWs are reviewed and presented in this section with particular focus on experimental results, demonstrating the potential of coupled resonator circuit architectures.

6.1. Applications in the linear regime

In the linear regime, CROWs are attractive for both their intrinsic wavelength-selective behavior and their ability to control the velocity, and hence the delay, of light pulses. Because of these properties, CROWs have been employed in the realization of high-performance optical filters and reconfigurable integrated delay lines, as discussed in Sects. 6.1.1 and 6.1.2, respectively.

6.1.1. CROW optical filters

High-order wavelength division multiplexing filters and add/drop multiplexers based on directly coupled ring resonators can exhibit a very high off-band rejection, while having passbands with a flat-top profile [38,41,58,110,128,130]. A CROW filter is realized by employing a conventional architecture with two input/output bus waveguides, as depicted schematically in Fig. 8a. In Fig. 8b the spectral response measured at the drop port of filters with an increasing number of resonators fabricated using high-index-contrast glass Hydex technology (see Fig. $5c_2$) is shown [41]; as the order of a filter increases, its spectral response approaches a box-like shape and the off-band rejection exceeds 80 dB for the eleventh-order filter. Bandwidths ranging from a few gigahertz to several hundreds of gigahertz have been successfully demonstrated, depending on the bending radius allowed by the fabrication technology [41, 58].

Ring CROWs offer design flexibility and the possibility of reconfiguring a filter response after fabrication. The parameters of CROW filters can be designed to match target intensity and group delay responses by applying synthesis algorithms similar to those used for microwave and digital filters [6, 28, 55, 76, 139–141]. Moreover, active tuning of the resonances of the rings and of the inter-ring coupling coefficients via embedded thermo-optic control, nonlinear thermal effects, carrier injection/depletion, or other activation strategies can allow the reconfiguration of the filter response during operation.

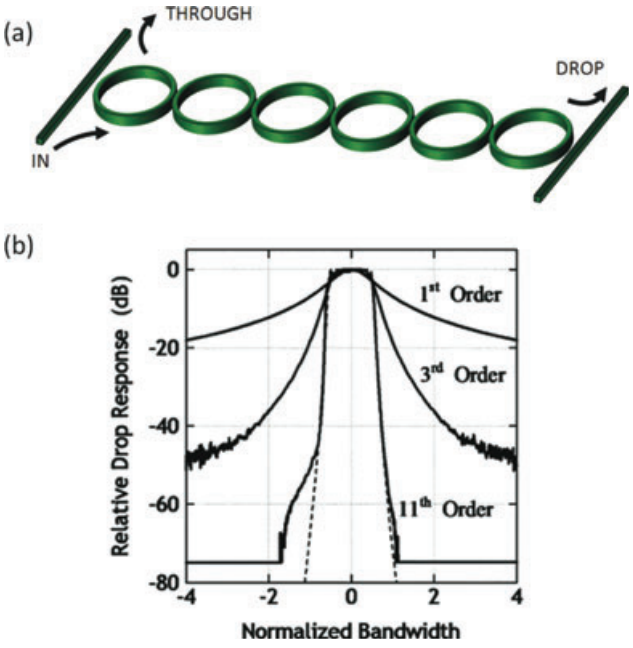

Figure 8 (online color at: www.lpr-journal.org) Application of CROWs as wavelength division multiplexing filters. (a) Schematic of a CROW filter consisting of a chain of ring resonators coupled with two bus waveguides. (b) Measured spectral response at the drop port for first-, third-, and eleventh-order microring resonator filters fabricated with Hydex technology. The responses have been normalized to their 3 dB bandwidths. The dashed curve is the theoretical fit to the eleventh-order filter. (Reproduced from [41] © 2004 IEEE.)

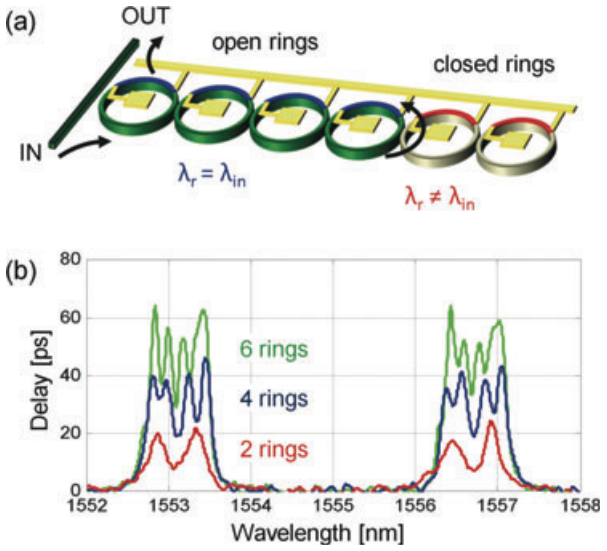

Figure 9 (online color at: www.lpr-journal.org) Application of CROWs as reconfigurable optical delay lines. (a) Schematic of a reconfigurable CROW delay line architecture with embedded metallization for thermal control of the resonances of the rings. (b) Measured group delay of the silicon CROW delay line of Fig. $5d_2$ when two, four, and six rings are opened. (Adapted from [64] © 2010 IEEE.)

6.1.2. CROW delay lines

As slow-light propagation gained increasing attention from the scientific community, it was suggested that the possibility of realizing all-optical buffers capable of temporarily storing information in the optical domain was among its most interesting applications [159]. The realization of devices for all-optical buffering is, indeed, the application where the properties of ring CROWs have found their most complete and advanced exploitation.

All-optical buffers can be of real interest for applications provided that a large delay, accounting for at least a few bit time slots, is induced on a modulated signal, by using devices with a wide operation bandwidth and with a compact and integrated architecture. The potential of CROWs to fulfill these requirements was immediately recognized and fixed delay lines based on CROWs were designed [160] and successfully demonstrated [58, 103]. Even with both a wide bandwidth and a significant delay (e.g. the silicon CROW buffer demonstrated by Xia et al. [58] induces a delay of 1 bit on a 5 Gbit/s signal), fixed CROW delay lines cannot be effectively exploited because of the lack of active control of the delay.

Starting from the scheme of the conventional CROW shown in Fig. 8a, a reconfigurable optical delay line can be achieved by conceptually "folding" the chain of resonators and removing one of the two bus waveguides. In this configuration, shown in Fig. 9a, the wavelength selectivity of the CROW is effectively exploited to introduce a gating mechanism that can dynamically modify the effective length of the structure, and hence the delay [43, 88]. A signal incoming from the bus waveguide is allowed to propagate through all the rings (colored green) of the chain that resonate at the carrier wavelength of the signal. Rings can be locked (gray rings) if set off-resonance with respect to the carrier wavelength of the signal; propagation through locked rings is prohibited and they act as mirrors to the lightwave signal. The signal backreflected by the first locked ring retraces its path towards the out port and exits the structure after having experienced a group delay which is directly proportional to the number of open rings.

Figure 9b shows the measured group delay of a silicon CROW delay line (the structure shown in Fig. $5d_2$) with bandwidth $B = 87$ GHz, finesse $F = 5$, and $S = 3$. By opening an increasing number of rings, the delay increases almost uniformly over the passing band, each ring providing an additional delay of 7.5 ps. Note that the bandwidth of the CROW is neither narrowed nor widened when the delay is adjusted. Some delay ripple within the passband is due to tolerance-induced nonoptimal impedance matching of the CROW (see Sect. 5.1).

Although the CROW delay line has a discrete structure, the last open resonator of the chain can be set in an intermediate state between the open and locked conditions in order to provide a continuously variable delay [88]. The structure can be successfully reconfigured by acting on a few rings only (usually two or three), which are sufficient to lock the signal propagation, independently of the overall length of the resonator chain. The need to actively tune only

a few resonators at a time to reconfigure the delay provides a remarkable advantage in terms of power consumption and management complexity over other resonator-based architectures that require accurate control of all the resonating elements [161, 162].

In the remainder of this subsection some key issues are discussed in detail to better point out the potential and the current limits of state-of-the-art CROW delay lines and of the technologies that can be used to realize these architectures.

Storage capacity. Reconfigurable CROW delay lines with storage capacities exceeding 1 byte (i.e. total delay greater than 8 bit time slots) have been demonstrated in both medium-index-contrast SiON glass and high-contrast silicon technologies [64,89]. The time traces of Fig. 10 show the measurement of 10 ps pulses, suitable for transmission at 100 Gbit/s, transmitted through a silicon CROW delay line (see Fig. $5d_2$) when an increasing number of resonators are opened. Because of the folded configuration, only 12 ring resonators are required for a 9-bit delay. Here, the rings are activated at 10 µs speed, by exploiting thermal control through embedded metallic heaters deposited onto the waveguides [65]. Similar results have been achieved in medium-index-contrast SiON CROW optical buffers at 10 and 25 Gbit/s [162]. The delay control resolution depends on the accuracy of the activation method; in the case of the thermo-optic effect, the absolute delay resolution is less than 1 ps in both glass and silicon structures.

Fractional loss. The fractional loss, i.e. the optical power lost per unitary bit delay, reveals what is often the most rigid constraint to the maximum storage capacity of integrated optical buffers. The theoretical limit to the minimum overall attenuation is strictly and exclusively related to the propagation loss exhibited by the waveguide technology and to the total delay, whereas it is independent of the circuit architecture of the buffer [88]. Loss versus delay in silicon CROWs is typically higher than in waveguides fabricated with lower index contrast technologies (see Sect. 4). In the silicon CROW of Fig. 10a, losses amount to about 0.06 dB/ps, whereas in SiON CROWs values as low as 0.01 dB/ps have been demonstrated [89]. This implies that SOI is an attractive technological platform to realize optical buffers at very high bit rates of 100 Gbit/s and beyond, where larger bandwidth and lower absolute delays are required; at slower data rates SOI is significantly outperformed by lower index contrast glass technologies. An interesting result is that at 100 Gbit/s silicon CROW delay lines exhibit approximately the same fractional loss (0.6 dB per bit delay of 10 ps) as SiON buffers working at 10 Gbit/s (1 dB loss per bit delay of 100 ps) [89].

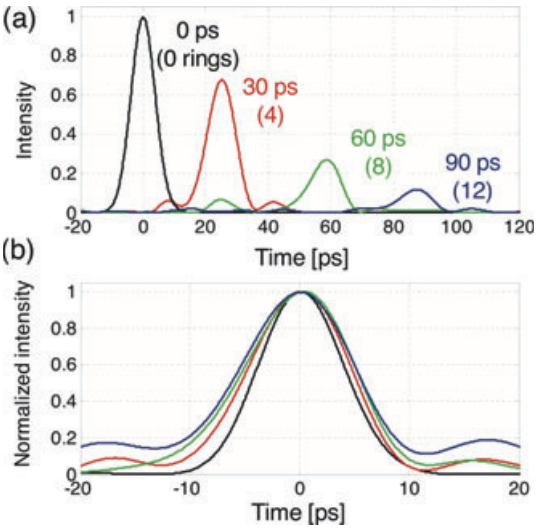

Figure 10 (online color at: www.lpr-journal.org) (a) Experimental demonstration of a silicon CROW delay line with 1 byte storage capacity at 100 Gbit/s. The time traces of delayed 10 ps Gaussian probe pulses are shown and delay is observed when 0, 4, 8, and 12 rings are open (on-resonance). (b) Superimposed and normalized envelopes of the delayed pulses shown in (a). (Adapted from [64] © 2010 IEEE.)

Chromatic dispersion. Theoretical predictions have often addressed chromatic dispersion as the most stringent limiting factor for the storage capacity of CROWs [163,164]. Although its effect is noticeable, experimental results reveal that it is not as constraining as losses [64, 89]. Figure 10b shows the normalized superimposed pulses of Fig. 10a, showing a visible but modest broadening ($< 20\%$), which causes slight intersymbol interference but does not prevent error-free transmission.

Storage efficiency. Another key figure of merit, which is an indicator of the bandwidth-delay product and of the management complexity of a buffering architecture, is the storage efficiency, defined as the number of bit pulses that are stored in each resonant element [88, 89]. A higher storage efficiency enables a reduction of the number of rings to be controlled for a given delay, thus simplifying the management of the structure and reducing electrical power consumption. However, there is an intrinsic limit to the maximum storage efficiency to avoid distortions in the buffered signal, this upper limit being roughly 1 bit per resonator in the folded scheme [89]. From this point of view, a CROW is a very effective architecture, if compared with other resonator-based configurations (e.g. all-pass architectures [58, 162]) proposed as integrated variable delay lines. Storage efficiencies very close to unity have been experimentally demonstrated in CROW delay lines, as in the structure of Fig. 10 exhibiting a storage efficiency of 0.75 bit per ring resonator. Storage efficiencies above 1 bit/ring can be achieved, yet at the cost of greater signal degradation [89].

Phase preservation. A fundamental requirement for devices employed in optical communication systems is transparency to modulation formats. Slow-light propagation in CROWs has been demonstrated to preserve information encoded in the phase of the optical field, and indeed no signal quality degradation is observed after transmission through a suitably designed CROW for intensity- and/or phase-modulated signals [64, 88, 166]. To give an example, Fig. 11a shows that the eye-diagram of an incoming 10 Gbit/s differential phase-shift-keying (DQPSK) signal is well preserved after propagation through an eight-ring silicon CROW [96].

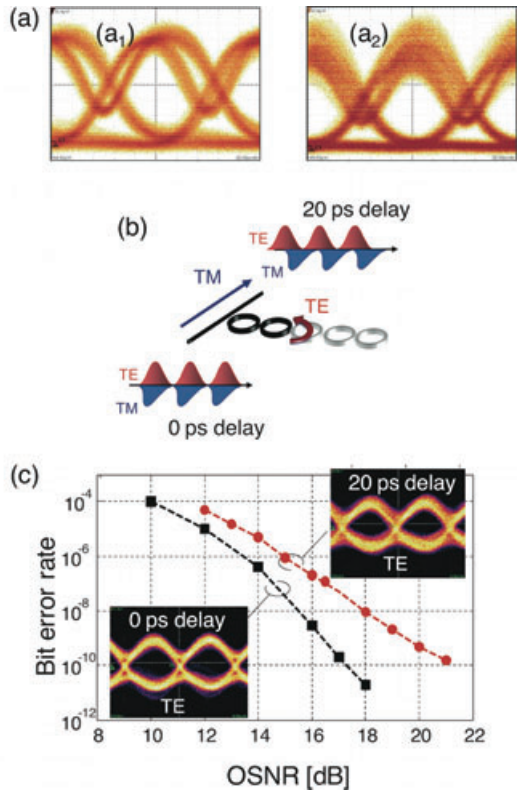

Figure 11 (online color at: www.lpr-journal.org) Phase-preserving transmission in CROWs. (a) Measured eye-diagrams of a 10 Gbit/s DPSK signal at the input (a_1) and at the output (a_2) of an eight-ring silicon CROW (reproduced from [96] ©2009 OSA). (b) Schematic of a polarization-selective reconfigurable CROW delay line (reproduced from [165] ©2009 IEEE). (c) Bit error rate measurements of a 100 Gbit/s DQPSK PolMux signal after propagation through a silicon polarization-selective CROW delay line: transverse electric performance when the two polarizations are time overlapped (0 ps relative delay, filled squares) and time interleaved (20 ps relative delay, filled circles) at the output of the device (adapted from [64] ©2010 IEEE).

Moreover, CROWs can be conveniently used to accomplish advanced processing tasks for arbitrarily complex modulation formats. Recently, a reconfigurable silicon CROW delay line was employed to control the mutual delay between the two orthogonally polarized channels of a 100 Gbit/s DQPSK polarization division multiplexed (PolMux) signal [64]. This device efficiently exploits the polarization sensitivity of the waveguide employed to realize the CROW. According to the scheme of Fig. 11b, only the transverse electric (TE)-polarized channel is coupled to the CROW and arbitrarily delayed with respect to the transverse magnetic (TM)-polarized channel that travels only in the bus waveguide [165]. Back-to-back bit error rate measurements of Fig 11c show that moving from time-overlapped polarization (CROW in locked state and no additional delay for TE polarization) to time-interleaved polarization (20 ps relative delay due to TE propagation through three rings of the CROW), error-free propagation (bit error rate of less than 10^{-9}) is preserved with a small penalty with respect to propagation in the bus waveguide only, demonstrating the low impact of the device on signal integrity.

Technology for CROW delay lines. Taking into account all the above-discussed quality parameters, low-loss medium-index-contrast glass technologies are very attractive for the realization of CROW delay lines operating at rates of a few tens of gigabits per second, where delays from hundreds of picoseconds to some nanoseconds are of interest. At these data rates, large rings with a radius of hundreds of micrometers (see Table 1) are suitable to maximize the storage efficiency and keep the fractional losses low, without involving strong technological challenges. High-index-contrast silicon microrings, with typical radii of less than 50 μm, would need a much higher finesse ($F > 50$) to achieve a comparable storage efficiency, but at the price of dramatically higher losses and challenging technological issues. The SOI platform becomes the leading technology at higher bit rates, where very large bandwidths and lower absolute delays are required. At 100 Gbit/s, silicon CROWs can reach storage efficiencies comparable to those of 10 Gbit/s SiON devices, with even lower fractional losses and similar finesse. Moreover, for silicon the efficiency of thermal control is enhanced by the higher thermo-optic coefficient and the typically smaller footprint of the devices (see Sect. 4).

These results show that CROW delay lines have reached a maturity level that makes them ready for exploitation in applications where the delay must be controlled with accuracy over a range of a few bit time slots. The maximum storage capacity of these devices is currently limited to a few tens of bits, the limiting factors being mainly related to losses and disorder (see Sect. 5), issues that have to be carefully considered and managed even for structures capable of inducing a short delay.

6.1.3. Other applications

Besides optical filters and delay lines, the wavelength selectivity of CROWs and the possibility to be reconfigured are attractive for a variety of other applications. A cascade of five silicon microring resonators was used to realize an ultra-compact ($40 \times 12\ \mu m^2$) wavelength-insensitive switch, capable of simultaneous error-free switching of a large number of high 40 Gbit/s bandwidth channels with minimal power penalties (< 0.3 dB) and robust against large temperature variations (up to 30 °C peak-to-peak) [44]. The switching mechanism employed is based on free-carrier injection into the silicon microrings by laser pumping at 488 nm, but in principle the rings can be activated using integrated PIN diodes embedded into the waveguides, as demonstrated for silicon optical modulators [45, 167, 168]. Fast activation of CROWs is a subject that still needs to be investigated in depth, but first results show that it can really open the way to new applicative horizons, as discussed in Sect. 7.

Other applications have been proposed for linear CROW structures, which aim to exploit the enhanced light-matter interaction associated with slow-light propagation. More than

a decade ago, pioneering works predicted [66] and experimentally demonstrated [77] the increase of the efficiency of electro-optic modulators assisted by slow-light propagation. In these applications, the reduction of the group velocity of the light has a twofold benefit: on the one hand, it provides an effective mechanism to match the velocity of the light to that of the microwave modulating signal, as required in lithium niobate wide-band traveling wave modulators [169]; on the other hand, owing to the increased dwelling time of the light in the structure, the strength of the electro-optic interaction scales up according to the slowdown factor S. A higher electro-optic efficiency can be exploited either to reduce the driving voltage of the modulator or to reduce the length of the electrodes, and hence to increase the bandwidth.

Enhanced light-matter interaction in CROWs has also been proposed for increasing the sensitivity of gyroscopes [170] and biochemical sensors for sensing nanoliter volumes [171] compared to nonresonant devices of the same footprint. Although promising, these applications are still at an embryonic stage and are not discussed in detail in this review.

6.2. Applications in the nonlinear regime

Among the nonlinear applications that have been proposed for CROWs, efficient wavelength conversion through cavity-enhanced FWM is one of the most appealing. As mentioned in Sect. 3, the efficiency of FWM conversion in resonant cavities is increased according to the fourth power of the slowdown factor (S^4) and has, therefore, been thoroughly investigated in single resonators fabricated with a wide range of nonlinear material platforms [50, 51, 82–87]. However the maximum conversion efficiency that can be achieved in single cavities is bound by a tight constraint between the bandwidth of the signal and the size of the resonator, the latter setting the length over which the nonlinear interaction takes place.

As pointed out in recent work [172], a single resonator behaves as a lumped nonlinear element (the concept of a lumped element being related to the pulse envelope rather than to its wavelength), since the pulse length must exceed the resonator length in order to avoid signal distortions. From this point of view, a CROW enables the extension of the traditional concept of cavity-enhanced FWM to a novel traveling wave approach. The number of cascaded resonators of a CROW can be increased with no bandwidth reduction, so that the propagation of a resonant optical field can cover a distance that is much longer than the pulse length. Propagation occurs as in conventional waveguides, but with both enhanced power and dwelling time, thus boosting any nonlinear interaction.

Traveling wave resonant FWM in CROWs has been demonstrated for the first time using SOI as a nonlinear platform. Figure 12a shows the spectral response at the drop port of a six-ring silicon CROW having an operational bandwidth of 100 GHz and FSR of 440 GHz [70]. The input signal has a TE polarization state. Figure 12b shows

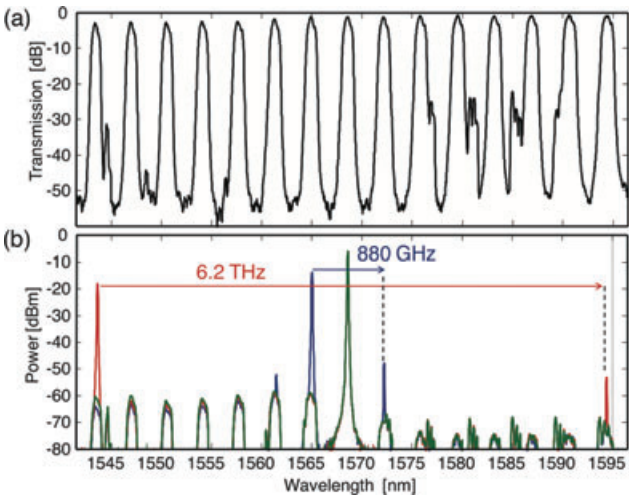

Figure 12 (online color at: www.lpr-journal.org) Wavelength conversion via cavity-enhanced FWM in silicon CROWs. (a) Transmission spectrum at the drop port of a six-ring silicon CROW with a bandwidth of 100 GHz and FSR of 440 GHz. (b) Spectrum at the drop port of the CROW of (a) showing wavelength conversion over 880 GHz (2 FSRs, blue curve) and over 6.2 THz (14 FSRs, red curve). The pump wave (green curve) is fixed at 1568.5 nm, the signal is tuned at 1565 nm (blue) and 1543.2 nm (red), and converted idlers are generated at 1572 and 1594.65 nm, respectively. (Adapted from [70] © 2009 OSA.)

the spectrum at the output of the device when a continuous pump wave propagates in the CROW passband centered at 1568.5 nm and a continuous signal wave propagates either inside an adjacent passband of the CROW, at 1565 nm, or inside a 25 nm-distant passband at 1543.52 nm. The generation of a converted idler at a wavelength of 1572 nm or 1594.65 nm demonstrates wavelength conversion over a range of 880 GHz and 6.2 THz, respectively, with no evident deterioration of the conversion efficiency over such a broad conversion range. The light exiting the CROW within each passband (about 20 dB below the idler spectrum) comes from the noise spectrum of the optical amplifiers used in the experiment. Note that the light lying in the stopbands is filtered out by the CROW, so that no spurious power contributions from and to these frequencies are generated.

Fig. 13a shows the advantage of traveling wave resonant FWM in a CROW with respect to a single resonator of the same bandwidth and FSR. Data points indicate the measured conversion efficiency for a single ring ($N = 1$) and for CROWs with six and eight rings. The power of the optical pump coupled into the bus silicon waveguide of each considered structure is 12 dB m. The conversion efficiency of the eight-ring CROW is 16 dB higher than that provided by the single resonator. This result confirms the quadratic dependence on the number of cascaded resonators predicted by Eq. (9), as is demonstrated by theoretical results shown in the figure for the case of null attenuation (dashed curve) and for 0.15 dB roundtrip losses within each resonator (solid curve).

A further advantage of a CROW with respect to a single resonator concerns the shape of the conversion band.

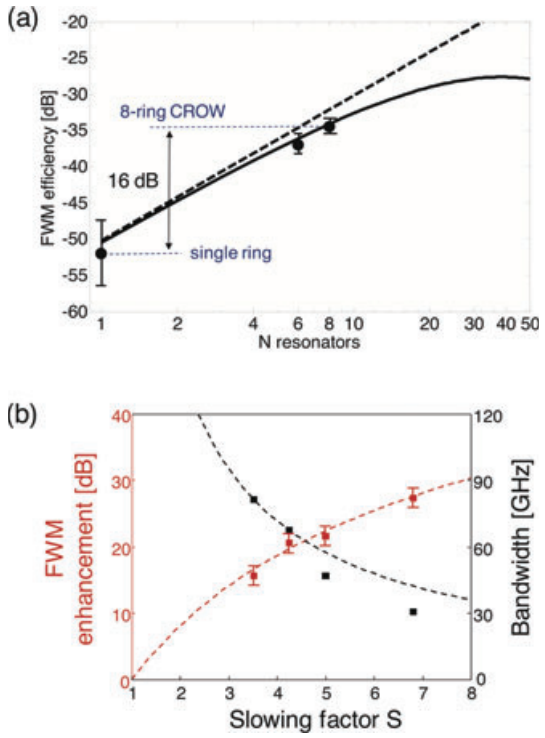

Figure 13 (online color at: www.lpr-journal.org) (a) Conversion efficiency of traveling wave FWM in silicon CROWs ($B = 80$ GHz and FSR = 450 GHz) versus the number N of resonators: experimental results (circles), and theoretical conversion efficiency in the absence of propagation loss (dashed curve) and in the case of 0.15 dB roundtrip loss in each ring (solid curve). (b) Conversion efficiency enhancement of eight-ring silicon CROWs ($L = 630$ μm) with respect to a silicon waveguide with the same physical length as a function of the slowdown factor S (red squares); black squares indicate the bandwidth of the measured CROWs. Dashed curves show the theoretical behavior. (Adapted from [172] © 2011 Macmillan Publishers Ltd.)

Owing to the flat-top transmission band of CROWs, the conversion efficiency is almost flat within the entire passband, preventing any intensity distortion [172]. In contrast, in single resonators both the signal and the converted waves are shaped according to the Lorentzian spectral response of the resonator, resulting in a significant reduction of the useful operation bandwidth.

The S^4 enhancement of the conversion efficiency with respect to a waveguide of the same length has been demonstrated [172] by realizing several CROWs with the same number of resonators ($N = 8$), the same physical length $L = 630$ μm, and FSR = 450 GHz, but different bandwidths, ranging from $B = 31$ to 81 GHz and with slowdown factors between $S = 3.5$ and 7. Red squares in Fig. 13b show that the measured enhancement of the conversion efficiency agrees well with the theoretical S^4 enhancement factor predicted by Eq. (9) (dashed curve). The corresponding CROW bandwidths are indicated by black squares. As a result, a slowdown factor $S = 7$ produces a conversion efficiency gain of 28 dB with respect to a bare waveguide of the same length, while maintaining a useful bandwidth of 30 GHz.

It should be noted that, with respect to photonic crystal waveguides, the slowdown of the light in CROWs is not associated with any mode shape variation. The impact of mode shape variations in photonic crystal waveguides with a similar $S \approx 7$ is responsible for a decrease of the conversion efficiency by 12 dB [173]. This reduction results from a fourfold increase of the mode size in the slow light regime with respect to the mode of a silicon nanowire. In contrast, in a CROW the S^4 enhancement is only limited by loss.

Results reported by Morichetti et al. [172] demonstrate also the following remarkable properties of traveling wave resonant FWM in CROWs: (1) it improves the robustness against chromatic dispersion and propagation loss with respect to conventional FWM in nonresonant waveguides, which is a direct consequence of the physical squeezing of the CROW, by a factor $(S^2 + 1)/2$, with respect to a straight waveguide with the same conversion efficiency; (2) it entirely preserves phase-encoded information and can be used for the all-optical processing of wide-band signals with arbitrarily complex modulation formats; and (3) it is compatible with any technological platform supporting the realization of integrated resonators and can be combined with alternative approaches that have been recently explored to improve the efficiency of nonlinear interactions, based for instance on optimized waveguide and material designs [174, 175].

7. Perspectives and outlook

The results discussed in the previous section demonstrate that CROWs have already found their place in many applications in the linear and nonlinear domain. However, the potential of CROWs does not stop there, because there are at least two other fields where CROWs are still waiting to be exploited: active domain and dynamic regime. In this concluding section, we try to envision some future directions with the help of a few pioneering works that opened new applicative horizons for CROWs.

Currently, waveguide loss is the primary issue that needs to be tackled to enable CROWs to realize their full potential. Amplification at the output is not a valuable solution, because losses weaken most of the phenomena enhanced by slow-wave propagation occurring inside the CROW. Losses must be cancelled *inside* the CROW. The problem could be circumvented by using active waveguides, where amplification can bring the waveguide to transparency or even provide a net gain. In the literature, only a few studies have been dedicated to the study of active CROWs, and, to the best of our knowledge, the only experimental results were obtained for active Fabry-Pérot resonator arrays fabricated in InP/InGaAsP [176, 177]. The theoretical study of active CROWs is a complicated task, because of the amplified spontaneous emission radiation that interacts with the signal, and because, above threshold, resonators can lock to each other and/or to the input signal, giving rise to complex phenomena that have been studied for decades in phase-locked laser arrays [178].

A particular property of active CROWs is that amplification occurs only within the passband, where waveguide

gain is enhanced according to S; any signal lying in the stopband is inherently filtered out, this preventing the generation of intermodulation effects and limiting the growth of background noise and, in general, of other spurious signals. Further, even if the signal-to-noise ratio does not improve within the passband with respect to classical optical amplifiers, the overall spontaneous emission is reduced, since noise generated in the stopband does not reach the output of the CROW. We believe that these aspects are all noteworthy and need to be accurately considered and developed in the near future.

CROWs in the dynamic regime have been the subject of intensive studies for stop light, trap light, time reversal, and frequency conversion phenomena. All these effects can originate when a resonator is dynamically perturbed, either at a slower or a faster speed than its natural time response (i.e. the inverse of the bandwidth), producing unique temporal and spectral modifications of the signal propagating inside. In the photonic crystals domain, pioneering works have been conducted by Reed et al. [179], Notomi and Mitsugi [180], and Preble et al. [181] concerning photonic crystal cavities and single-ring resonators and more recently by Kampfrath et al. concerning a slow-light photonic crystal waveguide [182]. The dynamics of time-varying CROWs is definitely more involved than that of single resonators, but it is enriched by unexpected phenomena that open unprecedented opportunities to manage and process optical signals.

As an example, Yanik and Fan [122] and subsequently Khurgin [124] have proposed different ways to break the delay-bandwidth product of a coupled resonator delay line by dynamically stopping, storing, and releasing light pulses. Figure 14a and b show the structures proposed in [124] and [122], respectively. In order to coherently stop a pulse with a given bandwidth, two conditions must be satisfied: (1) the system in its initial state must possess a sufficiently large bandwidth in order to accommodate the entire spectrum of the incoming pulse; and (2) the group velocity must be reduced to an arbitrarily low value while the pulse is entirely inside the system. This velocity change implicitly requires a frequency conversion mechanism of the signal, whose spectrum must be compressed in the process along with the structure bandwidth; information is preserved only if the frequency conversion process is adiabatic and reversible and the signal can be released without corrupting information. The adiabaticity requirements are related to the speed and the accuracy of the frequency shift of the resonators during the trap and release transitions and vary depending on the stop-light scheme that is adopted. The control of the activation of dynamic CROWs is a crucial issue, since stop-light schemes can be very sensitive even to small errors in the management of the resonators, which have the potential to heavily corrupt the shape of trapped light pulses.

Adiabatic light trapping and release can be accomplished in both structures as follows. In static conditions, that is while the pulse enters the structures, the resonance frequency of the rings matches the carrier frequency of the pulse. Soon after the pulse is completely loaded inside the structure, the resonance frequencies of some of the cavities

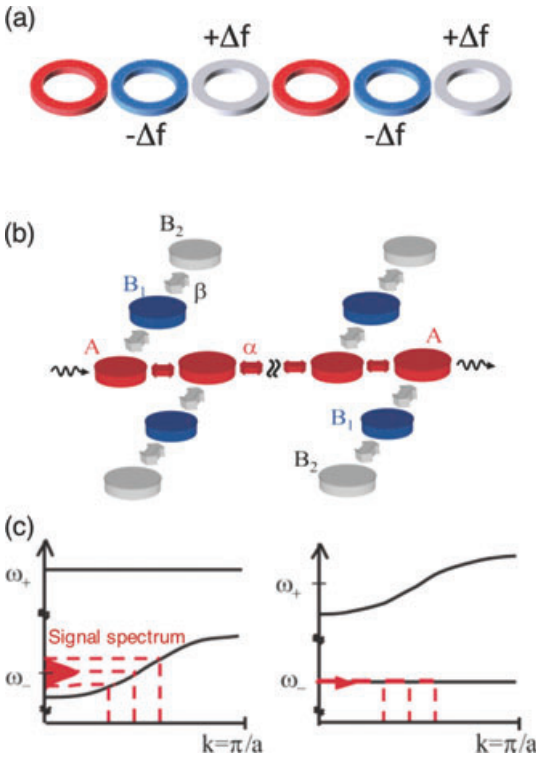

Figure 14 (online color at: www.lpr-journal.org) Dynamically tunable CROWs for stopping and trapping light. (a) An ordinary CROW whose resonators are periodically shifted by Δf to lower and higher resonance frequency [124]. (b) A cavity-loaded CROW structure consisting of a central chain of directly coupled low-Q resonators (red) which are side-coupled to (one or more) high-Q resonators (blue and grey). (c) Typical dispersion diagram of a dynamic CROW before light trapping (left) and in the trap state (right). The signal spectrum is squeezed and trapped in a state with almost null group velocity. (b, c) Reprinted with permission from [122] © 2004 American Physical Society.

are shifted, according to the adopted stop-light scheme, by changing the refractive index uniformly along the direction of propagation. Indeed, if the structure perturbation is translationally invariant, the wave vectors are preserved during the process and the spectrum is reversibly compressed in a state with almost null group velocity, as shown in Fig. 14c. The pulse can then be released by restoring the original state of the activated rings.

We have investigated stop-light phenomena through time-domain one-dimensional numerical simulations based on the transfer matrix method. Figure 15a shows a simulation of the space-time evolution of a 75 ps Gaussian pulse propagating along the ring-loaded CROW of Fig. 14b with a bandwidth of 30 GHz. The map shows the optical intensity in a chain of 100 low-Q central resonators represented as red discs in the figure. The pulse propagates through these resonators for 0.8 ns, then the structure is perturbed to trigger the stop-light process and light intensity is transferred to the lateral high-Q cavities (blue and grey), where it is trapped for 3 ns. After that the original CROW configuration is restored, the light reappears in the central rings, and the

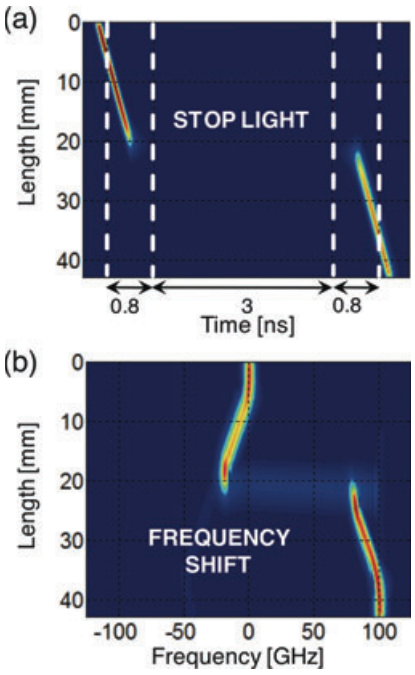

Figure 15 (online color at: www.lpr-journal.org) Simulation of (a) stop light and (b) frequency conversion in a dynamic ring-loaded CROW as in the scheme of Fig. 14b. The intensity maps show the evolution along the structure of (a) the time envelope and (b) the spectrum of a 75 ps Gaussian pulse propagating along a chain of 100 low-Q central resonators. After 0.8 ns the pulse is stopped and the energy is stored in the lateral resonators (it disappears in the map), while after 3 ns the pulse is released and it proceeds to propagate undistorted. In (b), the resonance frequencies of all the resonators are upshifted during the stop-light regime and the pulse spectrum is frequency shifted by 100 GHz after the release.

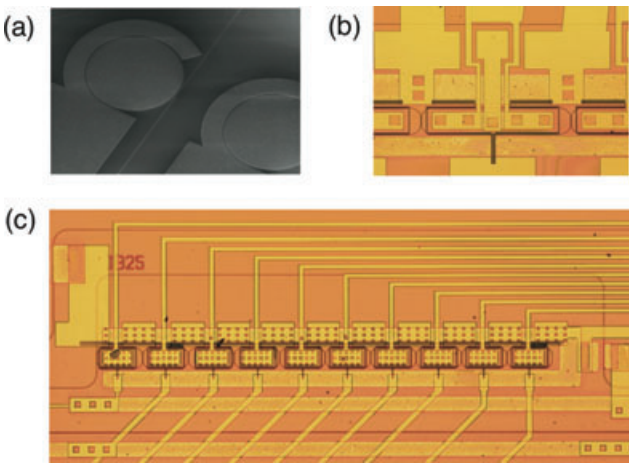

Figure 16 (online color at: www.lpr-journal.org) Dynamic silicon CROWs activated via PIN junctions. (a) Scanning electron micrograph of isolated ring resonators with PIN junctions embedded into the waveguide. (b) Detail and (c) overall view of a PIN junction-activated CROW made of 10 coupled racetrack resonators. The metal strips onto the chip realize the electric circuit for microsecond-scale thermal tuning and nanosecond-scale activation of the PIN junctions. Images are courtesy of University of Glasgow.

released light pulse keeps on propagating completely undistorted in the same direction towards the output port. In some architectures it is possible to make the released pulse propagate in the opposite direction with respect to the incoming pulse and achieve time reversal effects [183]. The effect of chromatic dispersion is dramatically reduced, or even eliminated, in the stop-light regime [184], while attenuation increases with the dwelling time into the structure, exactly as happens in conventional optical waveguides [185].

When a pulse is stopped, it can be manipulated by modifying some frequency and/or time characteristics. For instance, the signal spectrum can be rigidly shifted to a different carrier frequency without changing the pulse time envelope [186]. Both structures of Figs. 14a and b are suitable for this operation and the frequency shift Δf that can be induced obeys the simple law $\Delta f/f = \Delta n/n$, with Δn being the index perturbation. Figure 15b shows a simulation of frequency conversion assisted by stop-light in the same ring-loaded CROW of Fig. 15a. In the map the evolution of the spectrum of the input pulse along a chain of 100 low-Q central resonators is shown. After the stop-light and frequency-shift process, the output spectrum is rigidly upshifted by 100 GHz. It is worth noting that the frequency conversion occurs without the need for nonlinear material response and is therefore extremely appealing because it can be induced in any linear optical material whose refractive index can be rapidly modulated. Similar stop-light approaches have been recently investigated to achieve efficient optical amplification overcoming the gain-bandwidth constraint of slow-light systems [187].

Practical exploitation of dynamic CROWs requires fast activation of the waveguides on a time scale comparable to the duration of the optical pulse. Experiments to demonstrate the aforementioned effects have been planned and some prototypes have been already realized. Figure 16 shows the last frontier of silicon CROWs fabricated at the University of Glasgow. Each ring of the CROW is individually addressable by both thermal and electronic control: the first is used to finely tune the resonance wavelength and (re)configure the static response of the CROW; the second provides waveguide activation at sub-nanosecond speed by means of carrier injection in PIN junctions embedded into the waveguides.

Trap light, time reversal, frequency conversion, and spectral manipulation are only a few examples of fascinating effects that can be generated in a dynamic CROW. The full comprehension of the physics underlying such phenomena and the management of these structures, which are far away from being controllable devices, are challenging issues that have just been opened and are likely to attract significant interest and research effort in the near future.

Photonics is rapidly evolving towards increasingly more sophisticated integrated circuits, gathering many different optical elements and functionalities, and requiring accurate and reliable control. In this complicate and rapidly growing puzzle, CROWs are one of the last pieces that have been

added. Because of the maturity of integrated optics technology, it took only a decade to bring to reality what at first could be considered only a visionary dream. The potential of CROWs has been evaluated and exploited mostly in the scenario of optical communication, but in our belief CROWs are likely to pervade different fields of application, from sensing to biophotonics, from optical computing to optical interconnects, and many others. It is hard to predict where and when it will happen. What is certain now is that we are just at the beginning of the story.

Acknowledgements. The authors gratefully acknowledge Prof. M. Sorel, Prof. R. M. De La Rue, Dr. A. Samarelli, Dr. P. Velha, and all the technical staff of the James Watt Nanofabrication Centre at the University of Glasgow for the fabrication of some of the silicon devices described in this work. Many of the results reviewed in this paper were made possible by financial support within the EU6 project SPLASH and the British Council/MIUR British-Italian Partnership Programme 2009–2010 "SINAPSI".

Received: 15 March 2011, **Revised:** 16 May 2011, **Accepted:** 7 June 2011

Published online: 13 September 2011

Key words: Slow light, coupled resonators, optical cavities, optical waveguides, ring resonators, integrated optic technologies, integrated optical devices.

Francesco Morichetti received a PhD (summa cum laude) in information engineering in 2008 from Politecnico di Milano, Italy. From 2001 to 2008 he was a researcher in the integrated optic staff of the research consortium Corecom (Consortium for Research in Optical Signal Processing and Switching). Since 2009 he has been head of the Integrated Optic Lab at Policom, Politecnico di Milano. His research activity is focused on optical waveguides, photonic integrated circuits, and linear and nonlinear devices for optical signal processing. In the scientific community is considered one of the pioneers of the concept of optical slow-wave propagation. He is the author of three chapters of international books and of more than 100 publications in international journals and conference proceedings.

Carlo Ferrari received a PhD (summa cum laude) in information technology engineering in 2011 from Politecnico di Milano, Italy, defending a thesis on passive and nonlinear photonic integrated circuits for optical signal processing. During his PhD studies he temporarily joined Alcatel-Lucent Bell Labs in Murray Hill (NJ), USA, in an exchange program of nine months. His work on variable optical delay lines and efficient wavelength converters based on slow-light phenomena was carried out within the FP6 SPLASH project of the European Union.

Antonio Canciamilla received a PhD in information engineering from Politecnico di Milano, Italy, in 2010, with a dissertation on "Slow light structures for optical signal processing". From 2006 to 2008 he collaborated with the research consortium CoreCom and, since 2009, with Policom, Politecnico di Milano, where he has been temporary research fellow since 2010. His main research activities are modeling, design, and characterization of passive integrated optical components and circuits; slow-light structures and optical delay lines in the linear and nonlinear regime; silicon-on-insulator photonic waveguides and devices; and narrow-band optical filters for radio-frequency photonics. Since 2007 he has been involved in four F6 and F7 projects funded by the EU: SPLASH, NANOCAP, EuroPIC, and PARADIGM.

Andrea Melloni received a PhD in electronic and communication engineering at Politecnico di Milano, Italy, in 1992 with a thesis on microwave filters. In 1995 he joined the photonic group at Politecnico di Milano and since then his research interest has focused on integrated optical devices for optical communication systems. He is one of the pioneers of the slow-light concept and its exploitation in the linear and nonlinear domain using coupled cavities. From 2001 to 2008 he was an assistant at the research consortium CoreCom, Italy. In September 2008 he founded the company Filarete, for the development of ASPIC, the first circuit simulator for integrated optical circuits. He has been involved in the organization and steering of several conferences in the field of photonics and he is Topical Editor for JOSA A. Since 2003 he has been Associate Professor at Politecnico di Milano.

References

[1] Y. Yamamoto and R. E. Slusher, Phys. Today **46**(6), 66 (1993).
[2] K. J. Vahala, Nature **424**(6950), 839 (2003).
[3] K. J. Vahala, Optical Microcavities, Advanced Series in Applied Physics, Vol. 5 (World Scientific, 2004).
[4] I. Chremmos, O. Schwelb, and N. Uzunoglu, Photonic Microresonator Research and Applications, 1st edition, Springer Series in Optical Sciences, Vol. 156 (Springer, 2010).
[5] J. E. Heebner, R. Grover, and T. Ibrahim, Optical Microresonators: Theory, Fabrication, and Applications in Applied Physics, Springer Series in Optical Sciences, Vol. 138 (Springer, 2007).
[6] C. K. Madsen and J. Zhao, Optical Filter Design and Analysis: A Signal Processing Approach (John Wiley & Sons, 1999).
[7] D. G. Rabus, Integrated Ring Resonators: The Compendium, Springer Series in Optical Sciences, Vol. 127 (Springer, 2007).
[8] A. Yariv, Y. Xu, R. K. Lee, and A. Scherer, Opt. Lett. **24**(11), 711 (1999).

[9] Y. Xu, R. Lee, and A. Yariv, J. Opt. Soc. Am. B **17**, 387 (2000).
[10] A. Melloni, F. Morichetti, and M. Martinelli, Opt. Quantum Electron. **35**(4/5), 365 (2003).
[11] J. Khurgin and R. Tucker, Slow Light: Science and Applications (CRC Press Taylor & Francis, 2008).
[12] C. Fabry and A. Perot, J. Chim. Phys. **16**, 139 (1899).
[13] A. P. Alivisatos, Science **271**(5251), 933 (1996).
[14] W. Bogaerts, R. Baets, P. Dumon, V. Wiaux, S. Beckx, D. Taillaert, B. Luyssaert, J. Van Campenhout, P. Bienstman, and D. Van Thourhout, J. Lightwave Technol. **23**(1), 401 (2005).
[15] J. Hu, N. Carlie, N. Feng, L. Petit, A. Agarwal, K. Richardson, and L. Kimerling, Opt. Lett. **33**(21), 2500 (2008).
[16] J. Hu, A. Agarwal, L. Kimerling, N. Carlie, B. Zdyrko, L. Petit, I. Luzinov, and K. Richardson, Proc. Conf. Optical Fiber Communication (OFC), San Diego, CA (Optical Society of America, 2010), pp. 1–3.
[17] T. J. Kippenberg and K. J. Vahala, Opt. Express **15**(25), 17172 (2007).
[18] A. Schliesser, R. Riviere, G. Anetsberger, O. Arcizet, and T. J. Kippenberg, Nature Phys. **4**(5), 415 (2008).
[19] J. Scheuer, W. M. J. Green, G. DeRose, and A. Yariv, Opt. Lett. **29**(22), 2641 (2004).
[20] J. Scheuer, W. Green, G. DeRose, and A. Yariv, IEEE J. Sel. Top. Quantum Electron. **11**(2), 476 (2005).
[21] Y. Akahane, T. Asano, B. Song, and S. Noda, Nature **425**(6961), 944 (2003).
[22] J. Goeckeritz and S. Blair, Opt. Express **18**(17), 18190 (2010).
[23] P. Velha, E. Picard, T. Charvolin, E. Hadji, J. Rodier, P. Lalanne, and D. Peyrade, Opt. Express **15**(24), 16090 (2007).
[24] A. Zain, M. Gnan, H. Chong, M. Sorel, and R. M. De La Rue, IEEE Photon. Technol. Lett. **20**(1), 6 (2008).
[25] D. K. Armani, T. J. Kippenberg, S. M. Spillane, and K. J. Vahala, Nature **421**(6926), 925 (2003).
[26] M. L. Gorodetsky, A. A. Savchenkov, and V. S. Ilchenko, Opt. Lett. **21**(7), 453 (1996).
[27] M. L. Gorodetsky and V. S. Ilchenko, J. Opt. Soc. Am. B **16**(1), 147 (1999).
[28] B. E. Little, S. T. Chu, H. A. Haus, J. Foresi, and J. P. Laine, J. Lightwave Technol. **15**(6), 998 (1997).
[29] E. Marcatili, Bell Syst. Tech. J. **48**(7), 2103 (1969).
[30] R. G. Walker and C. D. W. Wilkinson, Appl. Opt. **22**(7), 1029 (1983).
[31] A. Mahapatra and W. C. Robinson, Appl. Opt. **24**(15), 2285 (1985).
[32] G. N. De Brabander, J. T. Boyd, and G. Beheim, IEEE Photon. Technol. Lett. **6**(5), 671 (1994).
[33] D. Rafizadeh, J. P. Zhang, S. C. Hagness, A. Taflove, K. A. Stair, S. T. Ho, and R. C. Tiberio, Opt. Lett. **22**(16), 1244 (1997).
[34] P. Rabiei, W. Steier, C. Zhang, and L. Dalton, J. Lightwave Technol. **20**(11), 1968 (2002).
[35] R. Grover, T. Ibrahim, T. Ding, Y. Leng, L. C. Kuo, S. Kanakaraju, K. Amarnath, L. Calhoun, and P. T. Ho, IEEE Photon. Technol. Lett. **15**(8), 1082 (2003).
[36] A. Melloni, R. Costa, P. Monguzzi, and M. Martinelli, Opt. Lett. **28**(17), 1567 (2003).
[37] J. Hu, N. Carlie, L. Petit, A. Agarwal, K. Richardson, and L. Kimerling, Opt. Lett. **33**(8), 761 (2008).
[38] T. Barwicz, M. Popovic, P. Rakich, M. Watts, H. Haus, E. Ippen, and H. Smith, Opt. Express **12**(7), 1437 (2004).
[39] B. Little, J. Foresi, G. Steinmeyer, E. Thoen, S. Chu, H. Haus, E. Ippen, L. Kimerling, and W. Greene, IEEE Photon. Technol. Lett. **10**(4), 549 (1998).
[40] A. Prabhu, A. Tsay, Z. Han, and V. Van, IEEE Photon. J. **2**(3), 436 (2010).
[41] B. E. Little, S. T. Chu, P. P. Absil, J. V. Hryniewicz, F. G. Johnson, F. Seiferth, D. Gill, V. Van, O. King, and M. Trakalo, IEEE Photon. Technol. Lett. **16**(10), 2263 (2004).
[42] P. Absil, J. Hryniewicz, B. Little, R. Wilson, L. Joneckis, and P. T. Ho, IEEE Photon. Technol. Lett. **12**(4), 398 (2000).
[43] F. Morichetti, A. Melloni, A. Breda, A. Canciamilla, C. Ferrari, and M. Martinelli, Opt. Express **15**(25), 17273 (2007).
[44] Y. Vlasov, W. M. J. Green, and F. Xia, Nature Photon. **2**(4), 242 (2008).
[45] Q. Xu, B. Schmidt, S. Pradhan, and M. Lipson, Nature **435**(7040), 325 (2005).
[46] M. T. Hill, H. J. S. Dorren, T. de Vries, X. J. M. Leijtens, J. H. den Besten, B. Smalbrugge, Y. Oei, H. Binsma, G. Khoe, and M. K. Smit, Nature **432**(7014), 206 (2004).
[47] A. Ksendzov and Y. Lin, Opt. Lett. **30**(24), 3344 (2005).
[48] M. Ferrera, Y. Park, L. Razzari, B. E. Little, S. T. Chu, R. Morandotti, D. J. Moss, and J. Azana, Nature Commun. **1**, 29 (2010).
[49] D. V. Thourhout and J. Roels, Nature Photon. **4**(4), 211 (2010).
[50] P. P. Absil, J. V. Hryniewicz, B. E. Little, P. S. Cho, R. A. Wilson, L. G. Joneckis, and P. Ho, Opt. Lett. **25**(8), 554 (2000).
[51] A. Pasquazi, R. Ahmad, M. Rochette, M. Lamont, B. E. Little, S. T. Chu, R. Morandotti, and D. J. Moss, Opt. Express **18**, 3858 (2010).
[52] L. Razzari, D. Duchesne, M. Ferrera, R. Morandotti, S. Chu, B. E. Little, and D. J. Moss, Nature Photon. **4**(1), 41 (2010).
[53] P. Yeh, A. Yariv, and C. Hong, J. Opt. Soc. Am. **67**(4), 423 (1977).
[54] R. E. Collin, Foundations for Microwave Engineering (McGraw-Hill, 1992).
[55] A. Melloni and M. Martinelli, J. Lightwave Technol. **20**(2), 296 (2002).
[56] A. Melloni, Opt. Lett. **26**(12), 917 (2001).
[57] J. E. Heebner, R. W. Boyd, and Q. Park, J. Opt. Soc. Am. B **19**, 722 (2002).
[58] F. Xia, L. Sekaric, and Y. Vlasov, Nature Photon. **1**(1), 65 (2007).
[59] M. Hossein-Zadeh and K. J. Vahala, IEEE J. Sel. Top. Quantum Electron. **16**(1), 276 (2010).
[60] A. M. Kapitonov and V. N. Astratov, Opt. Lett. **32**(4), 409 (2007).
[61] S. Mookherjea, J. S. Park, S. Yang, and P. R. Bandaru, Nature Photon. **2**(2), 90 (2008).
[62] T. Karle, D. Brown, R. Wilson, M. Steer, and T. Krauss, IEEE J. Sel. Top. Quantum Electron. **8**(4), 909 (2002).
[63] S. Olivier, C. Smith, M. Rattier, H. Benisty, C. Weisbuch, T. Krauss, R. Houdré, and U. Oesterlé, Opt. Lett. **26**(13), 1019 (2001).
[64] A. Melloni, A. Canciamilla, C. Ferrari, F. Morichetti, L. O'Faolain, T. F. Krauss, R. M. De La Rue, A. Samarelli, and M. Sorel, IEEE Photon. J. **2**(2), 181 (2010).

[65] A. Canciamilla, M. Torregiani, C. Ferrari, F. Morichetti, R. M. De La Rue, A. Samarelli, M. Sorel, and A. Melloni, J. Optics **12**(10), 104008 (2010).
[66] H. F. Taylor, J. Lightwave Technol. **17**, 1875 (1999).
[67] A. Melloni, F. Morichetti, and M. Martinelli, Opt. Photon. News **14**(11), 44 (2003).
[68] A. Melloni, F. Morichetti, and M. Martinelli, J. Opt. Soc. Am. B **25**(12), C87 (2008).
[69] A. Melloni, M. Torregiani, A. Canciamilla, and F. Morichetti, Proc. IEEE/LEOS Winter Topicals Meeting Series (IEEE/LEOS, 2009), pp. 148–149.
[70] F. Morichetti, A. Melloni, A. Canciamilla, C. Ferrari, M. Torregiani, A. Samarelli, R. M. De La Rue, and M. Sorel, Proc. Conf. Optical Fiber Communication (OFC), San Diego, CA (Optical Society of America, 2009), p. PDPA9.
[71] S. Mookherjea and A. Yariv, J. Sel. Top. Quantum Electron. **8**, 448 (2002).
[72] N. W. Ashcroft and N. D. Mermin, Solid State Physics (Harcourt Brace Jovanovich, 1976).
[73] J. Poon, J. Scheuer, S. Mookherjea, G. Paloczi, Y. Huang, and A. Yariv, Opt. Express **12**, 90 (2004).
[74] S. Mookherjea, D. S. Cohen, and A. Yariv, Opt. Lett. **27**, 933 (2002).
[75] W. J. Kim, W. Kuang, and J. O'Brien, Opt. Express **11**, 3431 (2003).
[76] R. Orta, P. Savi, R. Tascone, and D. Trinchero, IEEE Photon. Technol. Lett. **7**(12), 1447 (1995).
[77] N. Shaw, W. J. Stewart, J. Heaton, and D. R. Wight, Electron. Lett. **35**, 1557 (1999).
[78] J. E. Heebner and R. W. Boyd, Opt. Lett. **12**, 847 (1999).
[79] G. Agrawal, Nonlinear Fiber Optics, 4th edition (Academic Press, 2006).
[80] S. Mookherjea and A. Yariv, Phys. Rev. E **65**, 026607 (2002).
[81] S. Blair, Opt. Express **13**, 3868 (2005).
[82] J. Provost and R. Frey, Appl. Phys. Lett. **55**, 519 (1989).
[83] P. Bayvel and I. Giles, Electron. Lett. **25**, 1178 (1989).
[84] M. Fujii, C. Koos, C. Poulton, J. Leuthold, and W. Freude, IEEE Photon. Technol. Lett. **18**, 361 (2006).
[85] M. Ferrera, L. Razzari, D. Duchesne, R. Morandotti, Z. Yang, M. Liscidini, J. E. Sipe, S. Chu, B. E. Little, and D. J. Moss, Nature Photon. **2**(12), 737 (2008).
[86] A. Turner, M. Foster, A. Gaeta, and M. Lipson, Opt. Express **16**, 4881 (2008).
[87] J. S. Levy, A. Gondarenko, M. A. Foster, A. C. Turner-Foster, A. L. Gaeta, and M. Lipson, Nature Photon. **4**(1), 37 (2010).
[88] F. Morichetti, A. Melloni, C. Ferrari, and M. Martinelli, Opt. Express **16**(12), 8395 (2008).
[89] A. Melloni, F. Morichetti, C. Ferrari, and M. Martinelli, Opt. Lett. **33**(20), 2389 (2008).
[90] J. Poon, L. Zhu, G. DeRose, and A. Yariv, J. Lightwave Technol. **24**(4), 1843 (2006).
[91] L. C. Kimerling, L. Dal Negro, S. Saini, Y. Yi, D. Ahn, S. Akiyama, D. Cannon, J. Liu, J. G. Sandland, D. Sparacin, J. Michel, K. Wada, and M. R. Watts, in: Silicon Photonics, edited by D. J. Lockwood and L. PavesiTopics in Applied Physics (Springer, 2004), chap. 3.
[92] A. Melloni, R. Costa, G. Cusmai, and F. Morichetti, Int. J. Mater. Prod. Technol. **34**, 421 (2009).
[93] A. Melloni, R. Costa, G. Cusmai, F. Morichetti, and M. Martinelli, Proc. Workshop Fibres and Optical Passive Components (IEEE/LEOS, 2005), pp. 246–253.
[94] F. Morichetti, A. Canciamilla, C. Ferrari, M. Torregiani, A. Melloni, and M. Martinelli, Phys. Rev. Lett. **104**(3), 033902 (2010).
[95] F. Morichetti, A. Canciamilla, M. Martinelli, A. Samarelli, R. M. De La Rue, M. Sorel, and A. Melloni, Appl. Phys. Lett. **96**(8), 081112 (2010).
[96] F. Morichetti, C. Ferrari, A. Canciamilla, M. Torregiani, A. Melloni, A. Samarelli, R. M. De La Rue, and M. Sorel, Proc. Conf. Integrated Photonics and Nanophotonics Research and Applications, OSA Technical Digest (Optical Society of America, 2009), pp. 1–3.
[97] C. Ferrari, F. Morichetti, and A. Melloni, J. Opt. Soc. Am. B **26**(4), 858 (2009).
[98] S. Mookherjea and A. Oh, Opt. Lett. **32**(3), 289 (2007).
[99] M. A. Foster, A. C. Turner, M. Lipson, and A. L. Gaeta, Opt. Express **16**(2), 1300 (2008).
[100] C. Koos, L. Jacome, C. Poulton, J. Leuthold, and W. Freude, Opt. Express **15**(10), 5976 (2007).
[101] S. T. Chu, W. Pan, S. Sato, T. Kaneko, B. E. Little, and Y. Kokubun, IEEE Photon. Technol. Lett. **11**(6), 688 (1999).
[102] N. Carlie, J. D. Musgraves, B. Zdyrko, I. Luzinov, J. Hu, V. Singh, A. Agarwal, L. C. Kimerling, A. Canciamilla, F. Morichetti, A. Melloni, and K. Richardson, Opt. Express **18**(25), 26728 (2010).
[103] J. K. Poon, L. Zhu, G. A. DeRose, and A. Yariv, Opt. Lett. **31**(4), 456 (2006).
[104] F. Xia, L. Sekaric, M. O'Boyle, and Y. Vlasov, Appl. Phys. Lett. **89**(4), 041122 (2006).
[105] F. Xia, M. Rooks, L. Sekaric, and Y. Vlasov, Opt. Express **15**(19), 11934 (2007).
[106] T. Barwicz, M. A. Popovic, F. Gan, M. S. Dahlem, C. W. Holzwarth, P. T. Rakich, E. P. Ippen, F. X. Kartner, and H. I. Smith, Proc. SPIE, Lasers, Resonators and Beam Control no. 10, San Jose, CA (SPIE, 2008), pp. 68720Z.1–68720Z.12.
[107] M. A. Popovic, T. Barwicz, M. S. Dahlem, F. Gan, C. W. Holzwarth, P. T. Rakich, H. I. Smith, E. P. Ippen, and F. X. Kartner, Proc. 33rd European Conf. Optical Communication, Berlin, Germany (IEEE/LEOS, 2007), pp. 123–123.
[108] M. L. Cooper, G. Gupta, M. A. Schneider, W. M. J. Green, S. Assefa, F. Xia, Y. A. Vlasov, and S. Mookherjea, Opt. Express **18**(25), 26505 (2010).
[109] A. Melloni, F. Morichetti, G. Cusmai, R. Costa, A. Breda, C. Canavesi, and M. Martinelli,
Proc. 9th Int. Conf. Transparent Optical Networks (ICTON), Rome, Italy (IEEE/LEOS, 2007), pp. 223–226.
[110] A. Melloni, R. Costa, P. Monguzzi, and M. Martinelli, Opt. Lett. **28**(17), 1567 (2003).
[111] F. Morichetti, R. Costa, G. Cusmai, A. Cabas, M. Feré, M. C. Ubaldi, A. Melloni, and M. Martinelli, Proc. Conf. Optical Fiber Communication (OFC), Los Angeles, CA (Optical Society of America, 2004), p. FC8.
[112] Y. Yanagase, S. Yamagata, and Y. Kokubun, Electron. Lett. **39**(12), 922 (2003).
[113] P. Rabiei and W. Steier, IEEE Photon. Technol. Lett. **15**(9), 1255 (2003).
[114] J. K. S. Poon, Y. Huang, G. T. Paloczi, A. Yariv, C. Zhang, and L. R. Dalton, Opt. Lett. **29**(22), 2584 (2004).
[115] A. Agarwal, P. Toliver, R. Menendez, S. Etemad, J. Jackel, J. Young, T. Banwell, B. E. Little, S. T. Chu, W. Chen, W. Chen, J. Hryniewicz, F. Johnson, D. Gill, O. King, R. Davidson, K. Donovan, and P. J. Delfyett, J. Lightwave Technol. **24**(1), 77 (2006).

[116] J. Yang, N. K. Fontaine, Z. Pan, A. O. Karalar, S. S. Djordjevic, C. Yang, W. Chen, S. Chu, B. E. Little, and S. J. B. Yoo, IEEE Photon. Technol. Lett. **20**, 1030 (2008).
[117] M. Gnan, S. Thorns, D. S. Macintyre, R. M. De La Rue, and M. Sorel, Electron. Lett. **44**(2), 115 (2008).
[118] A. Khilo, M. A. Popovic, M. Araghchini, and F. X. Kartner, Opt. Express **18**(15), 15790 (2010).
[119] M. Pu, L. Liu, H. Ou, K. Yvind, and J. M. Hvam, Opt. Commun. **283**(19), 3678 (2010).
[120] D. Vermeulen, S. Selvaraja, P. Verheyen, G. Lepage, W. Bogaerts, P. Absil, D. Van Thourhout, and G. Roelkens, Opt. Express **18**(17), 18278 (2010).
[121] F. Gan, T. Barwicz, M. A. Popovic, M. S. Dahlem, C. W. Holzwarth, P. T. Rakich, H. I. Smith, E. P. Ippen, and F. X. Kartner, Proc. Conf. Photonics in Switching, San Francisco, CA (IEEE/LEOS, 2007), pp. 67–68.
[122] M. F. Yanik and S. Fan, Phys. Rev. Lett. **92**(8), 083901 (2004).
[123] M. Yanik and S. Fan, Phys. Rev. A **71**(1) (2005).
[124] J. Khurgin, Opt. Lett. **30**(20), 2778 (2005).
[125] Q. Lin, O. J. Painter, and G. P. Agrawal, Opt. Express **15**(25), 16604 (2007).
[126] H. K. Tsang, C. S. Wong, T. K. Liang, I. E. Day, S. W. Roberts, A. Harpin, J. Drake, and M. Asghari, Appl. Phys. Lett. **80**, 416 (2002).
[127] T. K. Liang and H. K. Tsang, Appl. Phys. Lett. **84**, 2745 (2004).
[128] J. V. Hryniewicz, P. P. Absil, B. E. Little, R. A. Wilson, and P. T. Ho, IEEE Photon. Technol. Lett. **12**(3), 320 (2000).
[129] D. Rabus, M. Hamacher, U. Troppenz, and H. Heidrich, IEEE J. Sel. Top. Quantum Electron. **8**(6), 1405 (2002).
[130] M. A. Popovc, T. Barwicz, M. R. Watts, P. T. Rakich, L. Socci, E. P. Ippen, F. X. Krtner, and H. I. Smith, Opt. Lett. **31**, 2571 (2006).
[131] B. J. Eggleton, B. Luther-Davies, and K. Richardson, Nature Photon. **5**(3), 141 (2011).
[132] X. Gai, T. Han, A. Prasad, S. Madden, D. Choi, R. Wang, D. Bulla, and B. Luther-Davies, Opt. Express **18**(25), 26635 (2010).
[133] M. W. Lee, C. Grillet, C. Monat, E. Mägi, S. Tomljenovic-Hanic, X. Gai, S. Madden, D. Choi, D. Bulla, B. Luther-Davies, and B. J. Eggleton, Opt. Express **18**(25), 26695 (2010).
[134] A. Zakery and S. R. Elliott, J. Non-Cryst. Solids **330**(1-3), 1 (2003).
[135] J. Hu, M. Torregiani, F. Morichetti, N. Carlie, A. Agarwal, K. Richardson, L. C. Kimerling, and A. Melloni, Opt. Lett. **35**(6), 874 (2010).
[136] A. Canciamilla, F. Morichetti, N. Carlie, J. D. Musgraves, B. Zdyrko, I. Luzinov, K. Richardson, J. Hu, V. Singh, A. Agarwal, L. C. Kimerling, and A. Melloni, Proc. European Conf. Lasers and Electrooptics (CLEO/Europe), Munich, Germany (IEEE, 2011), p. CE5.5.
[137] R. E. Collin, Field Theory of Guided Waves, 2nd edition (Wiley-IEEE Press, 1990).
[138] R. Biswas, Z. Y. Li, and K. M. Ho, Appl. Phys. Lett. **84**(8), 1254 (2004).
[139] K. Jinguji, J. Lightwave Technol. **14**(8), 1882 (1996).
[140] C. Madsen and J. Zhao, J. Lightwave Technol. **14**(3), 437 (1996).
[141] V. Van, J. Lightwave Technol. **24**(7), 2912 (2006).
[142] J. D. Domenech, P. Munoz, and J. Capmany, Opt. Express **17**, 21050 (2009).
[143] R. M. Fano, Theoretical Limitations on the Broadband Matching of Arbitrary Impedances, Technical Report, Research Laboratory Electronics, Vol. 41 (Massachusetts Institute of Technology, 1948).
[144] L. O'Faolain, T. P. White, D. O'Brien, X. Yuan, M. D. Settle, and T. F. Krauss, Opt. Express **15**(20), 13129 (2007).
[145] D. P. Fussell, S. Hughes, and M. M. Dignam, Phys. Rev. B **78**(14), 144201 (2008).
[146] S. Hughes, L. Ramunno, J. F. Young, and J. E. Sipe, Phys. Rev. Lett. **94**(3), 033903 (2005).
[147] S. G. Johnson, M. L. Povinelli, P. Bienstman, M. Skorobogatiy, M. Soljacic, M. Ibanescu, E. Lidorikis, and J. D. Joannopoulos,
Proc. 5th Int. Conf. Transparent Optical Networks (ICTON), Warsaw, Poland (IEEE/LEOS, 2003), pp. 103–109.
[148] D. Gerace and L. C. Andreani, Opt. Lett. **29**(16), 1897 (2004).
[149] E. Kuramochi, M. Notomi, S. Hughes, A. Shinya, T. Watanabe, and L. Ramunno, Phys. Rev. B **72**(16), 161318 (2005).
[150] R. J. P. Engelen, D. Mori, T. Baba, and L. Kuipers, Phys. Rev. Lett. **101**(10), 103901 (2008).
[151] L. O'Faolain, S. A. Schulz, D. M. Beggs, T. P. White, M. Spasenovic, L. Kuipers, F. Morichetti, A. Melloni, S. Mazoyer, J. P. Hugonin, P. Lalanne, and T. F. Krauss, Opt. Express **18**(26), 27627 (2010).
[152] B. E. Little, J. P. Laine, and S. T. Chu, Opt. Lett. **22**, 4 (1997).
[153] T. J. Kippenberg, S. M. Spillane, and K. J. Vahala, Opt. Lett. **27**, 1669 (2002).
[154] M. Borselli, T. Johnson, and O. Painter, Opt. Express **13**, 1515 (2005).
[155] C. Canavesi, F. Morichetti, A. Canciamilla, F. Persia, and A. Melloni, J. Lightwave Technol. **27**(15), 3062 (2009).
[156] M. L. Cooper, G. Gupta, J. S. Park, M. A. Schneider, I. B. Divliansky, and S. Mookherjea, Opt. Lett. **35**(5), 784 (2010).
[157] G. Priem, P. Dumon, W. Bogaerts, D. V. Thourhout, G. Morthier, and R. Baets, Opt. Express **13**(23), 9623 (2005).
[158] J. Leuthold, C. Koos, and W. Freude, Nature Photon. **4**(8), 535 (2010).
[159] R. S. Tucker, P. Ku, and C. J. Chang-Hasnain, J. Lightwave Technol. **23**(12), 4046 (2005).
[160] J. K. S. Poon, J. Scheuer, Y. Xu, and A. Yariv, J. Opt. Soc. Am. B **21**(9), 1665 (2004).
[161] M. Rasras, C. K. Madsen, M. Cappuzzo, E. Chen, L. Gomez, E. Laskowski, A. Griffin, A. Wong-Foy, A. Gasparyan, A. Kasper, J. L. Grange, and S. Patel, IEEE Photon. Technol. Lett. **17**(4), 834 (2005).
[162] N. K. Fontaine, J. Yang, Z. Pan, S. Chu, W. Chen, B. E. Little, and S. J. B. Yoo, J. Lightwave Technol. **26**(23), 3776 (2008).
[163] J. B. Khurgin, Opt. Lett. **32**(2), 133 (2007).
[164] J. B. Khurgin, Opt. Lett. **30**(5), 513 (2005).
[165] C. Ferrari, F. Morichetti, A. Canciamilla, A. Melloni, and M. Martinelli, IEEE Photon. Technol. Lett. **21**(20), 1541 (2009).
[166] A. Melloni, P. Boffi, C. Ferrari, L. Marazzi, F. Morichetti, R. Siano, and M. Martinelli, Proc. Conf. Optical Fiber Communication (OFC), San Diego, CA (Optical Society of America, 2009), pp. 1–3.
[167] B. Analui, D. Guckenberger, D. Kucharski, and A. Narasimha, IEEE J. Solid State Circuits **41**, 2945 (2006).

[168] W. M. J. Green, M. J. Rooks, L. Sekaric, and Y. A. Vlasov, Opt. Express **15**, 17106 (2007).
[169] R. Alferness, S. Korotky, and E. Marcatili, IEEE J. Quantum Electron. **20**, 301 (1984).
[170] M. Terrel, M. Digonnet, and S. Fan, Laser Photon. Rev. **3**(5), 452 (2009).
[171] H. Kurt and D. S. Citrin, Appl. Phys. Lett. **87**(24), 241119 (2005).
[172] F. Morichetti, A. Canciamilla, C. Ferrari, A. Samarelli, M. Sorel, and A. Melloni, Nature Commun. **2**(296), 1 (2011).
[173] J. Li, L. O'Faolain, I. H. Rey, and T. F. Krauss, Opt. Express **19**(5), 4458 (2011).
[174] M. Foster, A. C. Turner, J. E. Sharping, B. S. Schmidt, M. Lipson, and A. L. Gaeta, Nature **441**, 960 (2006).
[175] C. Koos, P. Vorreau, T. Vallaitis, P. Dumon, Bogaerts, R. Baets, B. Esembeson, I. Biaggio, T. Michinobu, F. Diederich, W. Freude, and J. Leuthold, Nature Photon. **3**, 216 (2009).
[176] J. K. S. Poon and A. Yariv, J. Opt. Soc. Am. B **24**(9), 2378 (2007).
[177] J. K. S. Poon, L. Zhu, J. M. Choi, G. A. De Rose, A. Scherer, and A. Yariv, J. Opt. Soc. Am. B **24**(9), 2389 (2007).
[178] W. W. Chow, S. W. Koch, and M. Sargent III, Semiconductor Laser Physics (Springer, 1994).
[179] E. J. Reed, M. Soljačić, and J. D. Joannopoulos, Phys. Rev. Lett. **90**(20), 203904 (2003).
[180] M. Notomi and S. Mitsugi, Phys. Rev. A **73**(5), 051803 (2006).
[181] S. F. Preble, Q. Xu, and M. Lipson, Nature Photon. **1**(5), 293 (2007).
[182] T. Kampfrath, D. M. Beggs, T. P. White, A. Melloni, T. F. Krauss, and L. Kuipers, Phys. Rev. A **81**(4), 043837 (2010).
[183] M. F. Yanik and S. Fan, Phys. Rev. Lett. **93**(17), 173903 (2004).
[184] S. Sandhu, M. L. Povinelli, M. F. Yanik, and S. Fan, Opt. Lett. **31**(13), 1985 (2006).
[185] C. Ferrari, VLSI photonic devices for all-optical signal processing, PhD thesis (Politecnico di Milano, 2011).
[186] F. Morichetti, C. Ferrari, and A. Melloni, Enhanced frequency shift in optical slow-wave structures, in: 9th Int. Conf. Transparent Optical Networks (ICTON), (2007), pp. 75–78.
[187] S. Sandhu, M. L. Povinelli, and S. Fan, Appl. Phys. Lett. **95**(8), 081103 (2009).